Published for SISSA by Springer

Received: November 4, 2015
Revised: February 11, 2016
Accepted: February 29, 2016
Published: March 17, 2016

Search for excited leptons in proton-proton collisions at $\sqrt{s} = 8$ TeV

The CMS collaboration

E-mail: cms-publication-committee-chair@cern.ch

Abstract: A search for compositeness of electrons and muons is presented using a data sample of proton-proton collisions at a center-of-mass energy of $\sqrt{s} = 8$ TeV collected with the CMS detector at the LHC and corresponding to an integrated luminosity of 19.7 fb^{-1}. Excited leptons (ℓ^*) produced via contact interactions in conjunction with a standard model lepton are considered, and a search is made for their gauge decay modes. The decays considered are $\ell^* \to \ell\gamma$ and $\ell^* \to \ell$Z, which give final states of two leptons and a photon or, depending on the Z-boson decay mode, four leptons or two leptons and two jets. The number of events observed in data is consistent with the standard model prediction. Exclusion limits are set on the excited lepton mass, and the compositeness scale Λ. For the case $M_{\ell^*} = \Lambda$ the existence of excited electrons (muons) is excluded up to masses of 2.45 (2.47) TeV at 95% confidence level. Neutral current decays of excited leptons are considered for the first time, and limits are extended to include the possibility that the weight factors f and f', which determine the couplings between standard model leptons and excited leptons via gauge mediated interactions, have opposite sign.

Keywords: Beyond Standard Model, Exotics, Hadron-Hadron scattering

ArXiv ePrint: 1511.01407

doi:10.1007/JHEP03(2016)125

Contents

JHEP03(2016)125

1 Introduction

The standard model (SM) of particle physics describes the observed phenomena very successfully, however it provides no explanation for the three generations of the fermion families. Attempts to explain the observed hierarchy have led to a class of models postulating that quarks and leptons may be composite objects of fundamental constituents [1–9]. The fundamental constituents are bound by an asymptotically free gauge interaction that becomes strong at a characteristic scale Λ. Compositeness models predict the existence of excited states of quarks (q^*) and leptons (ℓ^*) at the characteristic scale of the new binding interaction. Since these excited fermions couple to the ordinary SM fermions, they could be produced via contact interactions (CI) in collider experiments, with subsequent decay to ordinary fermions through the emission of a $\mathrm{W}/\mathrm{Z}/\gamma$ boson, or via CI to other fermions.

Searches at LEP [10–13], HERA [14], and the Tevatron [15–18] have found no evidence for excited leptons. At the Large Hadron Collider (LHC) at CERN, previous searches performed by the CMS [19] and the ATLAS collaborations [20] have also found no evidence of excited leptons, obtaining a lower limit on the mass $M_{\ell^*} < 2.2\,\mathrm{TeV}$ for the case $M_{\ell^*} = \Lambda$.

In this paper, a search for excited leptons (e^* and μ^*) is presented, using a data sample of pp collisions at a center-of-mass energy $\sqrt{s} = 8\,\mathrm{TeV}$ collected with the CMS detector at the LHC in 2012 and corresponding to an integrated luminosity of $19.7 \pm 0.5\,\mathrm{fb}^{-1}$ [21]. We consider the production of an excited lepton in association with an oppositely charged lepton of the same flavor, with subsequent radiative decays ($\ell\ell^* \to \ell\ell\gamma$) or neutral current decays ($\ell\ell^* \to \ell\ell\mathrm{Z}$).

2 Theory and model assumptions

The composite nature of quarks and leptons, if it exists, will manifest itself, above a characteristic energy scale Λ, as a spectrum of excited states. Such excited fermions, f^*, may couple to SM leptons and quarks via a four-fermion CI that can be described by the effective Lagrangian

$$\mathcal{L}_{\mathrm{CI}} = \frac{g_*^2}{2\Lambda^2} j^\mu j_\mu, \tag{2.1}$$

where Λ is the energy scale of the substructure, assumed to be equal to or larger than the excited fermion mass. The quantities $g_*^2 = 4\pi$, and j_μ, defined in ref. [7], involve only left-handed currents by convention. In addition to the coupling via CI, excited fermions can also interact with SM fermions via gauge interactions. For excited leptons, the corresponding Lagrangian for the gauge-mediated (GM) interaction is given by

$$\mathcal{L}_{\mathrm{GM}} = \frac{1}{2\Lambda} \bar{\mathrm{f}}_R^* \sigma^{\mu\nu} \left(g f \frac{\tau}{2} W_{\mu\nu} + g' f' \frac{Y}{2} B_{\mu\nu} \right) \mathrm{f}_L + h.c. \tag{2.2}$$

where $W_{\mu\nu}$ and $B_{\mu\nu}$ are the field-strength tensors of the SU(2) and U(1) gauge fields, and $g = e/\sin\theta_W$. The quantity, $g' = e/\cos\theta_W$ represents the electroweak gauge coupling with the Weinberg angle θ_W, and Y and τ are the generators of the U(1) and SU(2) groups, respectively. The quantities f_R and f_L are the right and left-handed components of the

JHEP03(2016)125

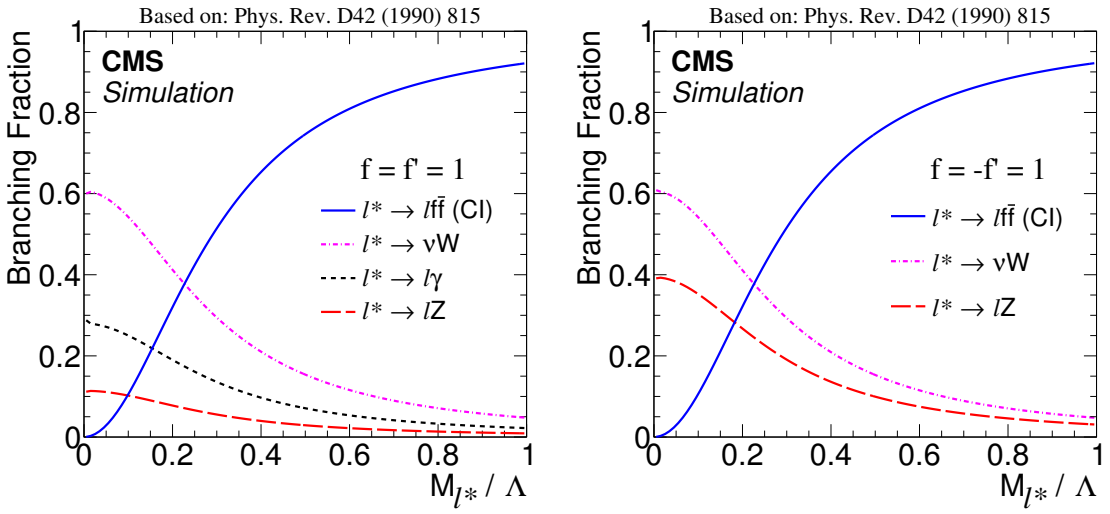

Figure 1. Branching fractions for the decay of excited leptons, as a function of the ratio M_{ℓ^*}/Λ of their mass to their compositeness scale, for the coupling weight factors $f = f' = 1$ (left) and $f = -f' = 1$ (right). The process $\ell^* \to \ell\bar{f}f$ indicates the decay via CI, while the other processes are gauge mediated decays.

lepton or excited lepton. The weight factors f and f' define the couplings between SM leptons and excited leptons via gauge interactions [7]. The compositeness scales contained in $\mathcal{L}_{\mathrm{CI}}$ and $\mathcal{L}_{\mathrm{GM}}$ are assumed to be the same.

The excited lepton, ℓ^*, can decay to a SM lepton via a CI $\ell^* \to \ell\mathrm{f}\bar{\mathrm{f}}$, where f is a fermion, or through the mediation of a gauge boson via a gauge interaction. The following gauge-interaction-mediated decays are possible: radiative decay $\ell^* \to \ell\gamma$, charged-current decay $\ell^* \to \ell'\mathrm{W}$, and neutral-current decay $\ell^* \to \ell\mathrm{Z}$. All four transitions, the CI and the three gauge interactions, are possible if $f = f'$, while $f = -f'$ forbids decays via photon emission. Since the exact relationship between the weight factors is unknown, the results are interpreted for two extreme values: $f = f' = 1$ and $f = -f' = 1$.

In the present analysis we search for the production of excited electrons and muons, e^* and μ^*, through a CI, which is dominant at the LHC for the model considered here. Excited leptons can also be produced via gauge interactions, but those processes involve electroweak couplings and contribute less than 1% to the cross section at the LHC; they have therefore been neglected here. For light ℓ^*, the decay of excited leptons via gauge interactions is dominant, while the decay via a CI becomes dominant at high masses, as shown in figure 1. The decay via a CI is not considered in the simulated samples used here.

The search channels considered in this analysis are summarized in table 1. The $\ell\ell^* \to \ell\ell\gamma$ final state is represented by the Feynman diagram in figure 2 left. A second class of searches seeks decays via the emission of a Z boson (figure 2 right), with the Z boson decaying to either a pair of electrons, a pair of muons, or a pair of jets. This decay mode allows the phase space where $f = -f'$, unexplored by previous LHC searches, to be investigated. The transverse momentum (p_{T}) of the Z boson coming from the decay of the excited lepton is larger for heavier excited-lepton masses, and at high p_{T} the final-

JHEP03(2016)125

Decay mode	Search channel	Notation
Radiative decay	$ee^* \to ee\gamma$	$ee\gamma$
$\ell\ell^* \to \ell\ell\gamma$	$\mu\mu^* \to \mu\mu\gamma$	$\mu\mu\gamma$
Neutral current $\ell\ell^* \to \ell\ell Z$	$ee^* \to eeZ \to 4e$	4e
	$ee^* \to eeZ \to 2e2\mu$	2e2μ
	$ee^* \to eeZ \to 2e2j$	2e2j
	$\mu\mu^* \to \mu\mu Z \to 4\mu$	4μ
	$\mu\mu^* \to \mu\mu Z \to 2\mu 2e$	2μ2e
	$\mu\mu^* \to \mu\mu Z \to 2\mu 2j$	2μ2j

Table 1. Final states for excited lepton searches considered in this analysis, where $\ell = e, \mu$. The notation for a specific channel is provided in the right most column. For neutral currents, the last two characters in this notation refer to particles from the decay of the Z boson.

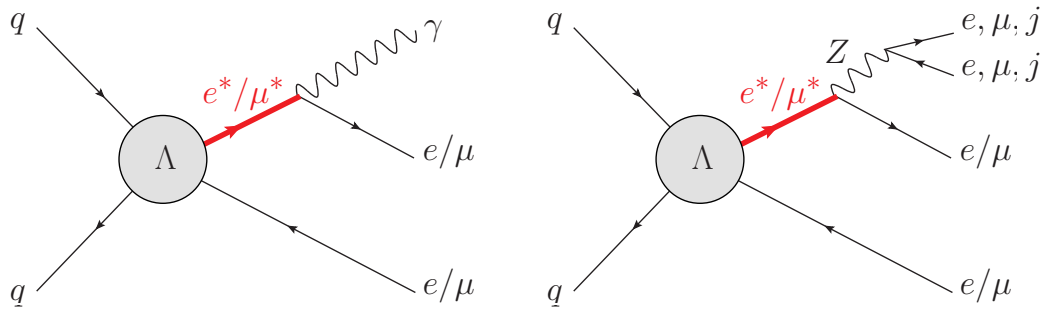

Figure 2. Illustrative diagrams for $\ell\ell^* \to \ell\ell\gamma$ (left) and $\ell\ell Z$ (right), where $\ell = e, \mu$. Decays of the Z boson to a pair of electrons, muons or jets are considered.

state particles are highly collimated. This characteristic is exploited in the $\ell\ell^* \to \ell\ell Z \to 2\ell 2j$ decay mode, in which jet substructure techniques are used to reconstruct a "fat jet" corresponding to the Z boson, and in the leptonic channels where the lepton isolation is modified.

Signal samples for both e^* and μ^* are produced using PYTHIA8.153 [22, 23], which uses the leading order (LO) compositeness model described in ref. [7]. Thirteen ℓ^* mass points from 200 to 2600 GeV have been simulated for all channels except the $\ell\ell jj$ channels, which starts at 600 GeV because of the analysis thresholds. Masses below 200 GeV are excluded by previous searches at 95% confidence level. All simulated events have been passed through the detailed simulation of the CMS detector based on GEANT4 [24] and have been re-weighted so that the distribution of pileup events (contributions from additional pp interactions in the same bunch crossing) matches that measured in data. The signal cross sections are calculated with PYTHIA8, and are corrected using the branching fraction to the 3-body decays via CI as predicted in ref. [7], as this decay mode is not implemented in PYTHIA. The factorization and renormalization scales are set to the mass square of the excited lepton ($M^2_{\ell^*}$), Λ is set to 10 TeV, and the CTEQ6L1 [25] parametrization for the

JHEP03(2016)125

parton distribution functions (PDF) is used. This particular choice of the value of Λ has no impact on the resulting kinematic distributions. Only the width of the ℓ^* resonance and the ℓ^* production cross section depend on Λ. As long as the width of the ℓ^* is small compared to the mass resolution of the detector, the signal efficiency is independent of Λ. Mass-dependent next-to-leading order (NLO) k-factors ranging from 1.2 to 1.35 [26] are applied on the signal event yields. Production cross sections for the signals, as well as those of the different decay modes including the corresponding branching fractions are given in table 2.

3 The CMS detector

The central feature of the CMS apparatus is a superconducting solenoid of 6 m internal diameter, providing a magnetic field of 3.8 T. Within the superconducting solenoid volume are a silicon pixel and strip tracker, a lead tungstate crystal electromagnetic calorimeter (ECAL), and a brass and scintillator hadron calorimeter (HCAL), each composed of a barrel and two endcap sections. Forward calorimeters extend the pseudorapidity (η) [27] coverage provided by the barrel and endcap detectors. Muons are measured in gas-ionization detectors embedded in the steel flux-return yoke outside the solenoid. In the barrel section of the ECAL, an energy resolution of about 1% is achieved for unconverted or late-converting photons in the tens of GeV energy range. The remaining barrel photons have a resolution of about 1.3% up to $|\eta| = 1$, rising to about 2.5% at $|\eta| = 1.4$. In the endcaps, the resolution of unconverted or late-converting photons is about 2.5%, while the remaining endcap photons have a resolution between 3 and 4% [28]. When combining information from the entire detector, the jet energy resolution amounts typically to 15% at 10 GeV, 8% at 100 GeV, and 4% at 1 TeV, to be compared to about 40%, 12%, and 5% obtained when the ECAL and HCAL calorimeters alone are used. The electron momentum is determined by combining the energy measurement in the ECAL with the momentum measurement in the tracker. The momentum resolution for electrons with $p_T \approx 45$ GeV from $Z \to ee$ decays ranges from 1.7% for non-showering electrons in the barrel region to 4.5% for showering electrons in the endcaps [29]. Muons are identified in the range $|\eta| < 2.4$, with detection planes made using three technologies: drift tubes, cathode strip chambers, and resistive plate chambers. Matching muons to tracks measured in the silicon tracker results in a relative p_T resolution for muons with $20 < p_T < 100$ GeV of 1.3–2.0% in the barrel and better than 6% in the endcaps. The p_T resolution in the barrel is better than 10% for muons with p_T up to 1 TeV [30]. A more detailed description of the CMS detector, together with a definition of the coordinate system used and the relevant kinematic variables, can be found in ref. [27].

4 Event selections

4.1 Triggers

The selected trigger for each channel is summarized in table 3. For all channels, except those with a 2e2μ final state, dilepton triggers are exploited: the double electron trigger

JHEP03(2016)125

Production cross sections for excited leptons				
M_{ℓ^*} (GeV)	LO σ (pb)			NLO k-factor
	$\Lambda = M_{\ell^*}$	$\Lambda = 4$ TeV	$\Lambda = 10$ TeV	
200	1.3×10^5	0.84	2.2×10^{-2}	1.30
1000	25.1	9.8×10^{-2}	2.5×10^{-3}	1.27
1800	0.28	1.1×10^{-2}	2.9×10^{-4}	1.28
2600	6.3×10^{-3}	1.1×10^{-3}	2.9×10^{-5}	1.35

$\sigma_{\mathrm{NLO}}\,\mathcal{B}\,(\ell\ell^* \to \ell\ell\gamma)$ (pb)						
M_{ℓ^*} (GeV)	$f = f' = 1$			$f = -f' = 1$		
	$\Lambda = M_{\ell^*}$	$\Lambda = 4$ TeV	$\Lambda = 10$ TeV	$\Lambda = M_{\ell^*}$	$\Lambda = 4$ TeV	$\Lambda = 10$ TeV
200	3.9×10^3	0.36	9.4×10^{-3}	—	—	—
1000	0.70	2.0×10^{-2}	8.0×10^{-4}	—	—	—
1800	7.7×10^{-3}	1.2×10^{-3}	7.5×10^{-5}	—	—	—
2600	1.9×10^{-4}	7.1×10^{-5}	6.0×10^{-6}	—	—	—

$\sigma_{\mathrm{NLO}}\,\mathcal{B}\,(\ell\ell^* \to \ell\ell\mathrm{Z} \to 2\ell 2\mathrm{j})$ (pb)						
M_{ℓ^*} (GeV)	$f = f' = 1$			$f = -f' = 1$		
	$\Lambda = M_{\ell^*}$	$\Lambda = 4$ TeV	$\Lambda = 10$ TeV	$\Lambda = M_{\ell^*}$	$\Lambda = 4$ TeV	$\Lambda = 10$ TeV
200	772	7.2×10^{-2}	1.9×10^{-3}	2.7×10^3	0.28	7.3×10^{-3}
1000	0.20	5.7×10^{-3}	2.3×10^{-4}	0.68	2.0×10^{-2}	7.8×10^{-4}
1800	2.2×10^{-3}	6.8×10^{-4}	2.1×10^{-5}	7.5×10^{-3}	1.2×10^{-3}	7.4×10^{-5}
2600	5.3×10^{-5}	2.0×10^{-5}	1.7×10^{-6}	1.8×10^{-4}	7.0×10^{-5}	5.9×10^{-6}

$\sigma_{\mathrm{NLO}}\,\mathcal{B}(\ell\ell^* \to \ell\ell\mathrm{Z} \to 2\ell 2\ell'$ ($\ell' = \mathrm{e}, \mu$)) (pb)						
M_{ℓ^*} (GeV)	$f = f' = 1$			$f = -f' = 1$		
	$\Lambda = M_{\ell^*}$	$\Lambda = 4$ TeV	$\Lambda = 10$ TeV	$\Lambda = M_{\ell^*}$	$\Lambda = 4$ TeV	$\Lambda = 10$ TeV
200	73.5	6.8×10^{-3}	1.8×10^{-4}	256	2.6×10^{-2}	6.9×10^{-4}
1000	1.9×10^{-2}	5.4×10^{-4}	2.1×10^{-5}	6.5×10^{-2}	1.8×10^{-3}	7.4×10^{-5}
1800	2.1×10^{-4}	3.4×10^{-5}	2.0×10^{-6}	7.2×10^{-4}	1.1×10^{-4}	7.0×10^{-6}
2600	5.0×10^{-6}	1.9×10^{-6}	1.6×10^{-7}	1.7×10^{-5}	6.6×10^{-6}	5.7×10^{-7}

Table 2. Excited lepton production cross section, and product of cross section and branching fraction for each of the three processes investigated, as a function of the mass of the excited lepton. The values of the k-factors are taken from ref. [26]. The case $f = -f' = 1$ does not apply to the $\ell\ell^* \to \ell\ell\gamma$ channel.

JHEP03(2016)125

Channel	Trigger	Offline p_T	Offline $\lvert\eta\rvert$	Signature and object ID
eeγ	Dielectron with 17(8) GeV	$E_T^{e1} > 35$ GeV, $E_T^{e2} > 35$ GeV, $E_T^{\gamma} > 35$ GeV	$\lvert\eta_e\rvert < 1.44$, $1.56 < \lvert\eta_e\rvert < 2.5$, $\lvert\eta_\gamma\rvert < 1.44$	Two isolated high E_T electrons and one isolated high E_T photon
$\mu\mu\gamma$	Dimuon with 17(8) GeV	$p_T^{\mu 1} > 35$ GeV, $p_T^{\mu 2} > 35$ GeV, $E_T^{\gamma} > 35$ GeV	$\lvert\eta_\mu\rvert < 2.1$, $\lvert\eta_\gamma\rvert < 1.44$	Two isolated high p_T muons and one isolated high E_T photon
2e2j	Dielectron with 17(8) GeV	$E_T^{e1} > 35$ GeV, $E_T^{e2} > 35$ GeV, $E_T^{j} > 200$ GeV	$\lvert\eta_e\rvert < 1.44$, $1.56 < \lvert\eta_e\rvert < 2.5$, $\lvert\eta_j\rvert < 2.4$	Two isolated high E_T electrons and two jets that are merged from boosted Z boson decays
2μ2j	Dimuon with 17(8) GeV	$p_T^{\mu 1} > 35$ GeV, $p_T^{\mu 1} > 35$ GeV, $E_T^{j} > 200$ GeV	$\lvert\eta_\mu\rvert < 2.4$, $\lvert\eta_j\rvert < 2.4$	Two isolated high p_T muons and two jets that are merged from boosted Z boson decays
4e	Dielectron with 17(8) GeV	$E_T^{e} > 25$ GeV for all four electrons	$\lvert\eta_e\rvert < 1.44$, $1.56 < \lvert\eta_e\rvert < 2.5$	Two isolated high E_T electrons and two nearby high E_T electrons from boosted Z boson decay, using modified isolation for Z boson decay electrons
2e2μ	Muon-Photon with 22 GeV each	$p_T > 25$ GeV for all four leptons	$\lvert\eta_e\rvert < 1.44$, $1.56 < \lvert\eta_e\rvert < 2.5$, $\lvert\eta_\mu\rvert < 2.4$	Two isolated high E_T electrons and two nearby high p_T muons from boosted Z boson decay, using modified ID for one Z boson decay muon and modified isolation for both Z boson decay muons
2μ2e	Muon-Photon with 22 GeV each	$p_T > 25$ GeV for all four leptons	$\lvert\eta_e\rvert < 1.44$, $1.56 < \lvert\eta_e\rvert < 2.5$, $\lvert\eta_\mu\rvert < 2.4$	Two isolated high p_T muons and two nearby high E_T electrons from boosted Z boson decay, using modified isolation for both Z boson decay muons
4μ	Dimuon with 17(8) GeV	$p_T^{\mu} > 25$ GeV for all four muons	$\lvert\eta_\mu\rvert < 2.4$	Two isolated high p_T muons plus two nearby high p_T muons from boosted Z boson decay, using modified ID for one and modified isolation for both muons from Z boson decay

Table 3. Trigger requirement, offline p_T and η-selection criteria, and event signature for all final state channels of the ℓ^* production and decay.

is used for events with electrons in the final state, while muon events are selected by the dimuon trigger. Both triggers have identical p_T thresholds, of 17 (8) GeV for the leading (subleading) lepton.

The two cross channels with 2e and 2μ in the final state exploit a muon-photon trigger with a p_T threshold of 22 GeV for both objects, where the photon trigger selects either electrons (as needed for this analysis) or photons, since the tracking information is not used

JHEP03(2016)125

at trigger level. The muon-photon trigger is chosen because the isolation requirements of the muon-electron trigger lead to an inefficiency when the two electrons from the Z boson decay are close together. The trigger efficiencies are close to one in all cases because of the large number of possible trigger objects. The offline p_{T} thresholds are set to 35 GeV for both electrons and muons, except for the 4-lepton channels, which require 25 GeV for each lepton.

4.2 Object reconstruction and selection

4.2.1 Electrons

Electron candidates are identified as clusters of energy deposited in the ECAL, associated with tracks measured with the silicon tracker [29]. The deposited energy should be predominantely in the electromagnetic calorimeter. Thus a lower limit is set on the ratio H/E where H stands for the energy deposited in the hadronic calorimeter and E for that in the electromagnetic calorimeter. These candidates must be within the barrel or endcap fiducial regions with $|\eta| < 1.44$ or $1.56 < |\eta| < 2.50$, respectively and have a $p_{\mathrm{T}} > 35$ GeV (25 GeV in the 4ℓ-searches). A set of identification requirements that are optimized for electrons with high transverse momenta [31], based on the profile of the energy deposition in the ECAL and the matching between the track and the cluster, are imposed to remove jets misidentified as electrons. The p_{T} sum of all other tracks (excluding the electron footprint) in a cone of $\Delta R = \sqrt{(\Delta\eta)^2 + (\Delta\phi)^2} < 0.3$ (where ϕ is the azimutal angle in radians) around the track of the electron candidate must be less than 5 GeV, a selection denoted as "tracker isolation". In computing the tracker isolation for electrons, tracks have to originate from within a distance $|d_{\mathrm{z}}| < 0.2$ cm from the primary vertex. This requirement reduces the impact of pileup interactions vetoing candidate events. The sum of the transverse energy (E_{T}) of calorimeter energy deposits in the same cone, referred to as "calorimeter isolation", must be less than 3% of the candidate's transverse energy. The calorimeter isolation energy is corrected for pileup by the subtraction of the average energy per unit area of (η, ϕ), computed for each event using the FastJet package [32].

For the two electrons from the Z boson decay (in the $\mathrm{ee}^* \to \mathrm{eeZ} \to 4\mathrm{e}$ and $\mu\mu^* \to \mu\mu\mathrm{Z} \to 2\mu 2\mathrm{e}$ channels), the tracker isolation and calorimeter isolation for each electron are modified to remove the contribution of the other electron [33].

4.2.2 Muons

The muon candidates have to pass identification (ID) criteria that are optimized for the reconstruction of muons with high transverse momenta [30, 31]. In the "global muon" reconstruction, muons are reconstructed within $|\eta| < 2.4$ by combining tracks from the inner tracker and the outer muon system. The following requirements are imposed: at least one hit in the pixel tracker; hits in more than five tracker layers; and the detection of the muon in at least two muon stations. Since the stations are separated by thick layers of iron, the latter requirement significantly reduces the probability of a hadron being misidentified as a muon. The relative uncertainty in the muon p_{T} measurement must not exceed 30%. In order to reduce the cosmic ray muon background, the transverse impact

JHEP03(2016)125

parameter of the muon track with respect to the primary vertex of the event is required to be less than 0.2 cm. The primary vertex is chosen as the one with the highest Σp_{T}^2 of all charged tracks associated with that vertex. Furthermore, the muon is required to be isolated by demanding that the scalar sum of the transverse momenta of all tracks, excluding the muon itself, within a cone of $\Delta R < 0.3$ around its own track, be less than 5% of its p_{T}.

In the $\mathrm{ee}^* \to \mathrm{eeZ} \to 2\mathrm{e}2\mu$ and $\mu\mu^* \to \mu\mu\mathrm{Z} \to 4\mu$ channels, one oppositely charged muon pair comes from the decay of the boosted Z boson. The muons can be close enough that one muon is inside the isolation cone of the other. Therefore, for these muons, the isolation calculation is modified by removing the contribution of the other muon. Also, the identification requirements on one of these muons are loosened: the global muon requirement is removed; the muon candidate is only required to be reconstructed in the tracker. After these modifications, the reconstruction and identification efficiency of nearby muons are found to be comparable to those of separated muons [33]. These two variations are referred to as "modified identification" and "relaxed isolation".

4.2.3 Photons

For photons, identification criteria from ref. [28] are applied to clusters in the ECAL that include requirements on the shower shapes, isolation variables, and H/E (ratio of deposits in the HCAL and ECAL in a cone around the photon direction). A photon candidate is required to have a cluster with $E_{\mathrm{T}} > 35$ GeV and to be in the barrel region of the ECAL, with $|\eta| < 1.44$. Photons are required to be in the central region because the jet-to-photon fake rate becomes high in the forward region, while only 4% of a signal would lie in this region. The photon is also required to be isolated within a cone of radius $\Delta R < 0.3$ both in the tracker and the calorimeter. The cone axis is taken to be the direction of the line joining the barycenter of the ECAL clusters to the primary vertex. The isolation criteria depend on the η of the photon, and distinguish between contributions from neutral and charged hadrons and electromagnetic particles. As with the electron isolation calculation, the sums do not include contributions from particles clearly associated with pileup vertices, and are adjusted for the estimated residual pileup.

4.2.4 Jets and $\mathrm{Z} \to \mathrm{jj}$ tagging

Hadronic jets are reconstructed from the list of particle flow (PF) candidates that are obtained with the PF algorithm [34, 34], which reconstructs and identifies single particles by combining information from all sub-detectors. Charged PF constituents not associated to the primary vertex are not used in the jet clustering procedure. Good PF candidates are clustered into jets using the Cambridge-Aachen (CA) algorithm [35] with a distance parameter $R = 0.8$. An area-based correction is applied, to take into account the extra energy clustered in jets from neutral particles in pileup interactions, using the FASTJET software package [32]. Jet energy corrections are derived from the simulation, and are validated with in-situ measurements using the energy balance of dijet, photon+jet, and Z+jets events [36]. Additional quality criteria are applied to the jets in order to remove spurious jet-like features originating from isolated noise patterns from the calorimeters or

JHEP03(2016)125

the tracker. These jet quality requirements are found to be 99% efficient for signal events. The jets are required to have $p_{\mathrm{T}} > 200\,\mathrm{GeV}$ and $|\eta| < 2.4$. Jets must also be separated from any well-identified lepton (passing selections of sections 4.2.2 and 4.2.1) by a cone of radius $\Delta R > 0.8$.

In the $2\ell 2\mathrm{j}$ channels, the search is optimized for high-mass excited leptons that produce a boosted, hadronically decaying Z boson. When such a highly boosted Z decays to two quarks, their separation is often so small that they are reconstructed as a single jet with a mass larger than that of a typical Quantum ChromoDynamics (QCD) jet. To achieve the best possible mass resolution for this single jet, a *jet pruning* algorithm [37, 38] is applied, which is also used by the CMS collaboration for several other physics analyses with hadronic decays of boosted W and Z bosons [33, 39–42]. This pruning procedure involves reclustering the constituents of the original jet and applying additional requirements to eliminate soft QCD radiation and large-angle QCD radiation coming from sources other than the Z boson. The kinematic distributions of the resultant jet are a closer reflection of the hard process. In particular, the pruned jet mass is closer to the mass of the parent Z boson.

In addition, to further discriminate against jets from gluon and single-quark hadronization, a quantity called N-subjettiness is used [43–45]. Before the pruning procedure is applied, the jet constituents are re-clustered with the k_{T} algorithm [46, 47], until N joint objects, called "subjets", remain in the iterative combination procedure of the k_{T} algorithm. The N-subjettiness, τ_N, is then defined as:

$$\tau_N = \frac{1}{\sum_k p_{\mathrm{T},k} R_0} \sum_k p_{\mathrm{T},k} \, \min(\Delta R_{1,k}, \Delta R_{2,k} ... \Delta R_{N,k}), \tag{4.1}$$

where the index k runs over the jet constituents and the distances $\Delta R_{n,k}$ are calculated with respect to the axis of the n^{th} subjet. The quantity R_0 is set equal to the jet radius of the original jet. The τ_N variable measures the capability of clustering the reconstructed particles in the jet in exactly N-subjets: if it has a small value then it represents a configuration that is more compatible with the N-subjettiness hypothesis. In particular, the variable that is best able to discriminate between the jets from a boosted Z boson decay and standard QCD jets is the ratio of 2- to 1-subjettiness, $\tau_{21} = \tau_2/\tau_1$. If the jet has $\tau_{21} < 0.5$ and if its pruned mass falls in the range between 70–110 GeV, the jet is tagged as originating from a Z boson, and is referred to as a "fat jet" in this paper.

The mismodeling of the τ_{21} variable can bias the signal efficiency estimated from the simulated samples. A discrepancy between data and simulation has been observed in the identification efficiency measured in events containing merged jets produced by boosted W-bosons from top decays that pass the same V-tag selections as the ones in this $\ell\ell$jj analysis [33]. Correction factors obtained from this sample are found to be 0.9 ± 0.1. These corrections are applied to the signal efficiencies obtained from simulation.

4.3 Signal selection

In addition to the trigger and object identification requirements, signal-candidate events are selected and SM backgrounds suppressed, sequentially as follows:

JHEP03(2016)125

1. Selection of final state objects (see section 4.3.1) and reconstruction of the boosted Z boson in those channels containing a Z boson.

2. Rejection of backgrounds with Z bosons (see section 4.3.2) with an invariant mass requirement.

3. Rejection of other backgrounds using a dedicated search window (see section 7.1) that uses two calculations of M_{ℓ^*}.

4.3.1 Preselection

As a first step, the final state objects are selected in the various search channels.

- $\ell\ell^* \to \ell\ell\gamma$: selection of two same flavor isolated leptons and one isolated high E_{T} photon within the acceptance and p_{T} thresholds given in table 3. In the case of $\mu\mu\gamma$, muon pairs that are back-to-back are rejected by removing those with an angle above $\pi - 0.02$ to avoid contributions from cosmic ray muons. Additionally, the muons are required to have opposite charges. Selected photons must be separated from the leptons by $\Delta R > 0.7$ to reduce the contribution from final state radiation.

- $\ell\ell^* \to \ell\ell\mathrm{Z} \to 2\ell 2\mathrm{j}$: selection of two isolated same flavor leptons and one fat jet (as defined in section 4.2.4) satisfying the acceptance and p_{T} thresholds given in table 3. If more than one fat jet is found, the one with the highest p_{T} is used. In the channel with muons, the muons are required to have opposite charges.

- $\ell\ell^* \to \ell\ell\mathrm{Z} \to 4\ell$: selection of exactly four isolated leptons (four electrons, four muons or two electrons and two muons) within the acceptance and p_{T} thresholds given in table 3. First, the relaxed ID (for muons) and isolation are used for all leptons. Next, the boosted Z boson is reconstructed. In the 2μ2e (2e2μ) channel, the electron (muon) pair defines the reconstructed Z boson. In the 4e and 4μ channels, the lepton pair with invariant mass closest to the Z pole mass is chosen. As a final step, the requirements on the leptons are tightened. In channels with the boosted Z boson decaying to muons, an additional charge requirement is applied to both muons, and one of the muons originating from the Z boson decay is allowed to fulfill the relaxed ID only; all other leptons need to pass the full ID.

The invariant mass of the two leptons (in the 4ℓ channels, of the two leptons that are not used to reconstruct the Z boson) is denoted as $M_{\ell\ell}$ in what follows. This di-lepton mass is used to reduce backgrounds that include Z bosons not associated with the decay of putative heavy leptons.

4.3.2 Invariant mass requirement

The invariant mass $M_{\ell\ell}$ is required to be above 106 GeV in the $\ell\ell\gamma$ and 4ℓ channels, and above 200 GeV for the $2\ell 2\mathrm{j}$ channels, to reduce backgrounds containing Z bosons. This cut efficiently removes contributions from $\mathrm{Z}\gamma$ (ZZ) to the $\ell\ell\gamma$ and the $2\ell 2\mathrm{j}$ backgrounds. For the eeγ channel, there is an additional Z-veto on the two possible electron-photon invariant

JHEP03(2016)125

masses to remove electron pairs coming from a Z decay, where one electron is misidentified as a photon. Events are removed where any of the electron-photon invariant masses is within $\pm 25\,\text{GeV}$ of the nominal Z boson mass.

5 Modeling of the background

5.1 Sources of background

Several SM processes contribute to the expected background for the various channels. Those contributions are discussed in the following.

- $\ell\ell^* \to \ell\ell\gamma$ channels: Drell-Yan (DY) production is the most important background for the $\ell\ell^* \to \ell\ell\gamma$ channels, mostly originating from production of a photon in association with a Z, which has a very similar signature to the signal. It is simulated using SHERPA1.4 [48] and its production cross section is normalized using a NLO cross section calculated with the Monte Carlo (MC) program MCFM6.1&6.6 [49, 50].

  Subleading contributions to the background arise from diboson events with an additional high energy photon or events in which an electron is misidentified as a photon. Such events are simulated using PYTHIA6.4 [23]. Background contributions also arise from events in which an additional prompt photon is produced together with a top pair ($t\bar{t}+\gamma$). These events are simulated with MadGraph5.1 [51] using a LO cross section. All these irreducible backgrounds arising from two prompt leptons and a prompt photon are estimated using MC simulation. Smaller contributions due to events with two genuine leptons and a jet which has been misidentified as a photon are estimated from data (see section 5.2). For the eeγ channel, jets faking electrons may contribute, although at a negligible level (see section 5.2.2 for details). The contribution of muons faked by jets is negligible.

- $\ell\ell^* \to \ell\ell Z \to 2\ell 2j$ channels: the production of a Z boson (decaying to leptons) plus additional jets is the dominant background followed by the production of two top quarks and diboson events. These contributions have been estimated from data, using simulation to validate the data-driven method described in section 5.2.3. All background contributions from simulation ($t\bar{t}$, diboson and DY+jets) are simulated using MadGraph with NLO cross sections that were calculated using MCFM.

- $\ell\ell^* \to \ell\ell Z \to 4\ell$ channels: the production of ZZ (including $Z\gamma^*$), with both bosons decaying leptonically, is the main background to the four-lepton channel and contributes about 90% of the total background expected. An additional smaller contribution arises from the production of three vector bosons where some of the leptons escape detection. The production of two top quarks, $t\bar{t}$, with or without an additional vector boson, can contribute to each channel. The background due to Higgs boson production is negligible in the phase space considered here. In the four lepton channels, all the backgrounds have been estimated using predictions from simulations. The $ZZ \to 4\ell$ background is described with GG2ZZ [52] for production via gluon fusion and in the case of $q\bar{q}$ annihilation at NLO with POWHEG1.0 [53–56].

JHEP03(2016)125

Processes involving $t\bar{t}$+X (X = W, Z, γ) and triple boson samples are simulated with MadGraph. It has been checked that the simulation describes correctly a sample of 4-lepton events selected as in section 4.3, but relaxing the Z-vetoes to increase the number of events.

Table 4 summarizes the simulated background samples with the corresponding NLO cross sections, and the channels where these samples are used. pythia has been used to perform the fragmentation and hadronization of samples generated with MadGraph. The pileup simulation has been re-weighted so that the distribution of pileup events matches that measured in data. All simulated events have been passed through the detailed simulation of the CMS detector based on Geant4 [24]. Correction factors are also applied to allow for differences between the simulated and measured reconstruction efficiencies of the physics objects.

5.2 Data-driven backgrounds

5.2.1 Misidentification of electrons

Backgrounds with zero or one real electron can contribute to the eeγ candidate sample. The largest contributions come from processes such as W($\rightarrow$ eν)+jet+γ where the jet in the event is misidentified as an electron. Misidentification can occur when photons coming from π^0 or η mesons inside a jet convert to an e^+e^- pair. Other possible sources include processes with a charged particle within a jet providing a track in the tracker and an electromagnetic cluster that together fake an electron signature, or a track from a charged particle that matches a nearby energy deposition in the calorimeter from another particle. The misidentification rate, $f^{\text{misid}}_{\text{electron}}$, is calculated as the ratio between the number of candidates passing the electron selection criteria with respect to those satisfying looser selection criteria. The looser criteria require only that the first tracker layer contributes a hit to the electron track and that loose identification requirements on the shower shape and the ratio H/E are satisfied. The misidentification rate is estimated as a function of E_{T} in bins of η using a data sample selected with a trigger requiring at least one electromagnetic cluster.

In order to estimate the contribution of misidentified electrons to the selected events, the misidentification rate is applied to a subsample of data events containing one electron passing good electron criteria and a second one passing a loose set of criteria. This loose set of criteria includes cuts on shower shape and the ratio H/E, but allows one of the electron selection criteria to be missed. The events are required to satisfy all other selection criteria of the analysis.

The systematic uncertainty in $f^{\text{misid}}_{\text{electron}}(E_{\text{T}}, \eta)$ is determined using a sample of events containing two reconstructed electrons as in [31]. The contribution from jet events to the inclusive dielectron mass spectrum can be determined either by applying the misidentification rate twice on events with two loose electrons or by applying the misidentification rate once on events with one fully identified electron and one loose electron. The first estimate lacks contributions from W+jets and γ+jets events while the second estimate is contaminated with DY events. These effects are corrected for using simulated samples. The

JHEP03(2016)125

Process	Selection	Generator	NLO cross section (pb)	Channel
Z+jets $\to \ell\ell$+jets	$p_{\mathrm{T}}^{\mathrm{Z}} = 70$–$100\,\mathrm{GeV}$	MADGRAPH	5.30×10^4	$2\ell 2\mathrm{j}$
Z+jets $\to \ell\ell$+jets	$p_{\mathrm{T}}^{\mathrm{Z}} > 100\,\mathrm{GeV}$	MADGRAPH	3.92×10^4	$2\ell 2\mathrm{j}$
W+jets $\to \ell\nu$+jets	—	MADGRAPH	3.63×10^4	$2\ell 2\mathrm{j}$
$\mathrm{Z}\gamma \to \ell\ell\gamma$	$\Delta R(\gamma,\ell) > 0.6$	SHERPA	14.9	$\ell\ell\gamma$
$\mathrm{t\bar{t}}$+jets	—	MADGRAPH	23.9	$2\ell 2\mathrm{j}$
$\mathrm{t\bar{t}}\gamma$	$E_{\mathrm{T}}(\gamma) > 10\,\mathrm{GeV}$	MADGRAPH	1.44(LO)	$\ell\ell\gamma$
$\mathrm{t\bar{t}Z}$	—	MADGRAPH	0.208	4ℓ
$\mathrm{t\bar{t}W}$	—	MADGRAPH	0.232	4ℓ
$\mathrm{WW} \to 2\ell 2\nu$	—	MADGRAPH	6.03	$2\ell 2\mathrm{j}$
WW	—	PYTHIA6	54.8	$\ell\ell\gamma$
$\mathrm{WZ} \to 2\ell 2\mathrm{q}$	—	MADGRAPH	2.32	$2\ell 2\mathrm{j}$, 4ℓ
$\mathrm{WZ} \to 3\ell\nu$	—	MADGRAPH	1.00	$2\ell 2\mathrm{j}$, 4ℓ
WZ	—	PYTHIA6	33.2	$\ell\ell\gamma$
$\mathrm{ZZ} \to 2\ell 2\mathrm{q}$	—	MADGRAPH	2.47	$2\ell 2\mathrm{j}$, 4ℓ
$\mathrm{ZZ} \to 2\ell 2\nu$	—	MADGRAPH	0.71	$2\ell 2\mathrm{j}$
$\mathrm{ZZ} \to 4\ell$	—	MADGRAPH	0.177	$2\ell 2\mathrm{j}$
ZZ inclusive	—	PYTHIA6	17.7	$\ell\ell\gamma$
$\mathrm{ZZ} \to 4\ell$	—	POWHEG	0.077	4ℓ
$\mathrm{ZZ} \to 2\ell 2\ell'$	—	POWHEG	0.176	4ℓ
$\mathrm{gg} \to \mathrm{ZZ} \to 4\ell$	—	GG2ZZ	0.005	4ℓ
$\mathrm{gg} \to \mathrm{ZZ} \to 2\ell 2\ell'$	—	GG2ZZ	0.012	4ℓ
WWZ	—	MADGRAPH	0.063	4ℓ
WZZ	—	MADGRAPH	0.020	4ℓ
ZZZ	—	MADGRAPH	0.005	4ℓ

Table 4. Background samples with the corresponding generator and cross sections used for the various channels. Specific generator selections are shown where important for the interpretation of the quoted cross sections.

observed difference of 30% between the two estimates is taken as the systematic uncertainty in the jet-to-electron misidentification rate.

5.2.2 Misidentification of photons

Hadronic jets in which a π^0 or η meson carries a significant fraction of the energy may be misidentified as isolated photons. Thus Z+jet(s) events are a potential background for the $\ell\ell\gamma$ search. The photon misidentification rate is measured directly from data using a data set collected using a single photon trigger. To avoid trigger biases, the events must contain at least one reconstructed super-cluster (energy deposit in the ECAL) besides the one that fired the trigger. In addition, the ratio of hadronic energy to the energy of that super-

JHEP03(2016)125

cluster is required to be less than 5%. The misidentification rate is defined as the ratio of the number of photon candidates that pass all the photon selection criteria (numerator) to the ones that pass a loose set of shower shape requirements but fail one of the photon isolation criteria (denominator). The numerator sample can have a contribution from isolated true photons. The contamination is estimated using the distribution of energy-weighted shower width computed in units of crystal lateral dimension. The shower shape for isolated true photons is obtained from a simulated sample. The shape of non-isolated photons is obtained from data by considering a background dominated region (side-band region) of the photon isolation variable. The true photon fraction in the numerator is estimated by fitting these two different shower shapes (signal and background templates) to the shower shape distribution of the numerator sample. The photon misidentification rate is calculated in photon E_{T} bins. It decreases with increasing photon E_{T} and is at most of the order of a few percent. As an example, for photons of $E_{\mathrm{T}} = 100\,\mathrm{GeV}$ the jets-to-photon misidentification rate is about 1.5%.

In order to estimate the contribution of misidentified photons to the selected events, the misidentification rate is applied to a subsample of data events that satisfy all selection criteria listed in section 4.3 except that the photon candidate must pass a looser set of shower shape requirements and fail one of the photon isolation criteria.

There are two main sources of uncertainties in the determination of jet to photon misidentification rate. First, the shower shape of non-isolated photons is obtained from data in the side band region: changing the side band region results in some change in the template for non-isolated photons. Second, the probability for a jet to fake a photon is different for quark and gluon jets and the fraction of jets due to quarks may not be the same in the sample used to obtain the fake rate and in the sample where this fake rate is applied. Considering these two sources of uncertainties, a conservative systematic uncertainty of 50% is assigned, independently of the photon E_{T}.

5.2.3 Data-driven background in 2ℓ2j

The backgrounds due to DY+jets, $\mathrm{t\bar{t}}$ and di-boson production are estimated using the "ABCD" method, which relies on two variables to separate the signal from the background. The two-dimensional plane of these two variables is divided in four disjoint rectangular regions A, B, C, and D, so that the region A is the signal region, while B, C, and D are the control regions, dominated by backgrounds. If the ratio of the backgrounds in regions A and B is the same as that for C and D (which holds if the two variables are independent), i.e.: $N_{\mathrm{A}}/N_{\mathrm{B}} = N_{\mathrm{C}}/N_{\mathrm{D}}$, then the background in the signal region A, N_{A} can be estimated as:

$$N_{\mathrm{A}} = N_{\mathrm{C}}\frac{N_{\mathrm{B}}}{N_{\mathrm{D}}}, \tag{5.1}$$

where N_{A}, N_{B}, N_{C}, and N_{D} are the background events in regions A, B, C, and D, respectively. The variables exploited in this analysis are the dilepton invariant mass $M_{\ell\ell}$ and N-subjettiness τ_{21}. The region A is defined by the selection cut given in sections 4.2.4 and 4.3. The regions B, C and D correspond to a similar selection but with reversed

JHEP03(2016)125

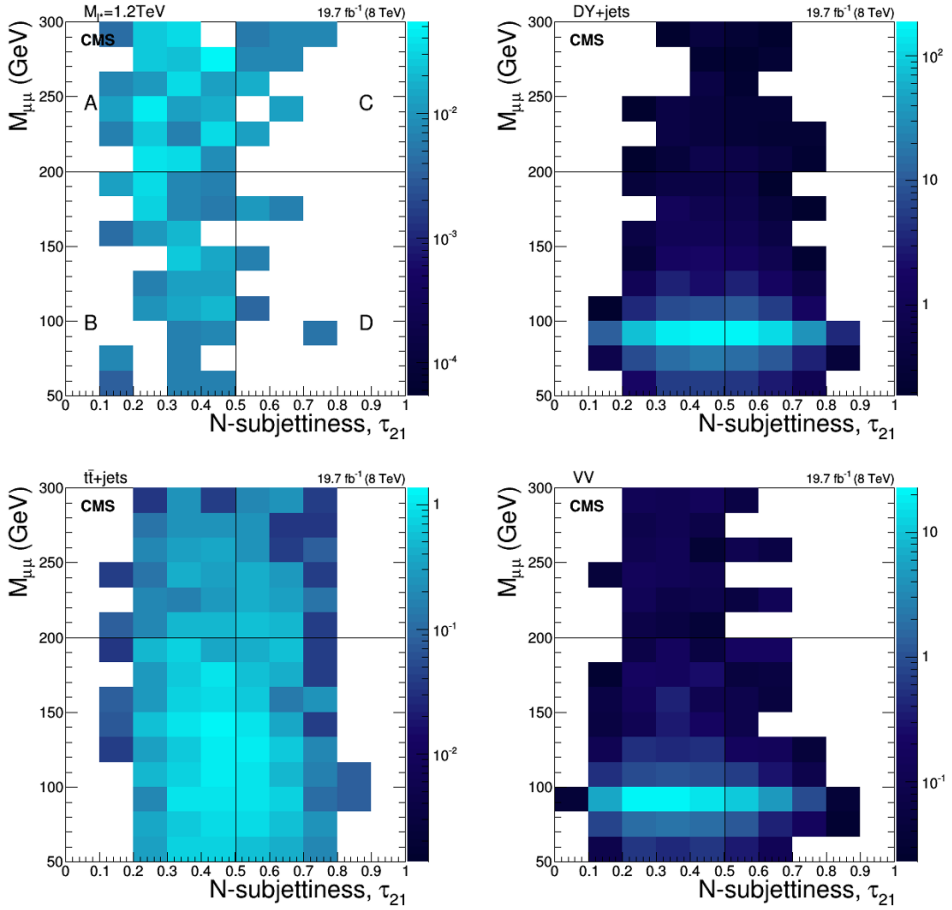

Figure 3. Invariant mass of the pair of isolated muons vs. the N-subjettiness ratio, τ_{21}, of the selected fat jet, for events passing the selection criteria given in section 4.3, but with the cuts on $M_{\ell\ell}$ and τ_{21} relaxed for signal with $M_{\ell^*} = 1.2\,\text{TeV}$ (top left), Drell-Yan+jets (top right), $\text{t}\bar{\text{t}}$+jets (bottom left) and diboson events (bottom right). The right hand scale gives to the number of events corresponding to the given integrated luminosity and the respective cross sections of the processes.

requirements on $M_{\ell\ell}$ and/or on the subjettiness ratio τ_{21} of the selected highest p_{T} fat jet. These four regions are indicated in figure 3 (upper-left) along with the borders of the regions (shown as solid lines) corresponding to the invariant mass $M_{\ell\ell}$ being either above (for signal) or below (for background) 200 GeV and τ_{21} being either above (background) or below (signal) 0.5.

For the 2μ2j final state, figure 3 shows background and signal predictions as a function of the invariant mass of the pair of isolated muons and the N-subjettiness ratio, τ_{21}, of the fat jet but without selection on τ_{21}. The background events displayed are from simulated samples of DY+jets, $\text{t}\bar{\text{t}}$+jets, and diboson production, while the signal events are from a sample simulated at $M_{\ell^*} = 1.2\,\text{TeV}$. In the signal region A, about 20 background events are expected, with ∼50% originating from DY+jets and ∼40% due to $\text{t}\bar{\text{t}}$+jets.

Several tests were performed using simulated samples to verify that the ABCD method using these variables reliably predicts the background yield. The relation given in Equation 5.1 is expected to be independent of the choice of boundaries for the control regions.

JHEP03(2016)125

Thresholds ($M_{\ell\ell}$, τ_{21})	From simulation estimated N_A	From data estimated N_A
muon channel		
(200, 0.50)	19.3 ± 1.4	20.9 ± 5.6
(180, 0.52)	19.8 ± 1.6	23.9 ± 6.4
(160, 0.54)	20.2 ± 1.8	20.4 ± 6.4
electron channel		
(200, 0.50)	16.6 ± 1.3	22.1 ± 5.9
(180, 0.52)	16.3 ± 1.3	24.2 ± 6.8
(160, 0.54)	16.6 ± 1.5	23.9 ± 7.2

Table 5. Events estimated in the region A by applying the ABCD method to simulated samples of DY+jets, $t\bar{t}$+jets, and di-boson events, as well as to data: each time with a different set of defining boundaries for regions B, C and D. The true number of events in region A is 19.2 ± 1.3 and 15.0 ± 1.1 for the muon and electron channel, respectively.

This assumption has been tested by applying the ABCD method to simulated samples of DY+jets, tt+jets and di-boson events. Moving the boundaries of regions B, C and D changed the calculated number of events in region A (whose definition is kept fixed) only slightly, as shown in table 5.

6 Systematic uncertainties

Three types of systematic uncertainties are considered:

- *Overall uncertainties in the simulation:* these include the uncertainty in the luminosity [21], the simulation of pileup and uncertainties in the cross sections used. These uncertainties affect the normalization and are treated similarly for all background- and signal simulations.
- *Object simulation uncertainties:* these depend on the final state of the respective analysis and are applied to the simulation of signal and background events. They consist, for example, of uncertainties in the energy or momentum scale and resolution of the various particles, or in correction factors that were applied to account for differences between the simulated and the actual performance of the detector.
- *Uncertainties in background estimations from data:* these uncertainties are applied to background components that were estimated from data and are only relevant to the $\ell\ell^* \to \ell\ell\gamma$ and $\ell\ell^* \to \ell\ell Z \to 2\ell 2j$ channels.

The sources of these systematic uncertainties are discussed in section 6.1 and their implications for signal and background in section 6.2.

6.1 Object-specific simulation uncertainties

Electron uncertainties. For electrons, uncertainties exist for the electron energy scale and electron identification efficiency. In both the barrel and the endcap, the scale uncer-

JHEP03(2016)125

tainties are determined by shifting the transverse energy of the electrons by 0.3% [29]. Systematic uncertainties due to electron identification are 2% and 4% [31] for very high energy electrons in barrel and endcap, respectively.

Muon uncertainties. There are three sources of uncertainties for muons: uncertainties in the muon momentum scale; the muon momentum resolution; and the efficiency of the muon selection. As described in ref. [30] the uncertainty in the muon momentum scale is estimated to be $5\% \times p_{\mathrm{T}}/\,\mathrm{TeV}$ and the effect of the scale uncertainty is estimated by changing the p_{T} by this value. The uncertainty in the muon momentum resolution is 0.6% and the effect of this uncertainty is estimated by smearing the p_{T} of the muons by an additional 0.6%. The uncertainty in the selection efficiency is 0.5% for the identification criteria, and 0.2% for the isolation criterion for each muon.

Photon uncertainties. The energy scale and resolution uncertainties for photons are very small compared to those of the other objects. The energy scale uncertainties are determined by shifting the transverse energies of the photons by 0.15% in the barrel section of the calorimeter [28].

Jet-energy scale. Jet-energy corrections are applied to account for the response function of the combined calorimeter system and other instrumental effects, based on in situ measurements using dijet, Z+jet, and photon+jet data samples [36]. Uncertainties due to these corrections are evaluated by shifting the jet energies by the calibration uncertainties ($\pm 1\sigma$). The effect on signal yield was found to be less than 1%.

6.2 Implications of uncertainties on signal and background yield

The above sources of uncertainties are specifically associated with the simulation of the various objects. To quantify each uncertainty on the signal and background, the relevant quantity is varied by $\pm 1\sigma$, relative to the best estimate. Subsequently all kinematic selections are reapplied and the impact on the analysis is determined by calculating the difference of the result from that of the original parametrization.

For all channels, the impact of pileup uncertainties was estimated by shifting the mean number of additional interactions and the inelastic cross section by 5%. The uncertainty in the signal yield cross section is taken to be 10%, following ref. [26].

In the case of the four lepton final states, the dominant uncertainty in the background is the uncertainty in the cross section of the ZZ background, which is conservatively assumed to be 15% ([57]). Additional uncertainties with a large impact on the background yield are the electron energy scale (with impact on background yield of 12%), the electron selection efficiency (6%), and the uncertainty in the electron resolution (2.5%). The mixed channels suffer large effects from the electron energy scale (8%), electron efficiencies (5%), and muon efficiencies (3%). In the four muon channel, the second largest uncertainty is associated with the muon selection efficiency (4%) followed by that on the muon momentum scale (1.6%). In this channel the uncertainties in the signal yield are completely dominated by the corresponding cross section uncertainty.

JHEP03(2016)125

In the $\ell\ell^* \to \ell\ell\gamma$ channel, the dominant systematic uncertainty in the background is the uncertainty in the production cross section arising from the parametrization of the parton distribution functions in the main background ($Z\gamma$), which was determined to be 10% by changing the choice of PDF set in the simulation according to ref. [58, 59]. Although the uncertainty in the data-derived background was determined to be 50%, its impact is rather small (4%), as the total contribution of this background is rather small. The impact of the photon energy scale and resolution are negligible. One of the dominant systematic uncertainties for the signal in the $\mu\mu^* \to \mu\mu\gamma$ channel is that in the muon momentum scale [30], which rises with increasing p_{T}. As a result, the impact on the final event yield is rather small in case of the background, containing muons of moderate momenta, but reaches more than 5% in the high-mass signal samples.

In the $\ell\ell^* \to \ell\ell\mathrm{Z} \to 2\ell 2\mathrm{j}$ channel, the dominant systematic uncertainty in the background is that associated with the background estimation method, mainly the signal contamination in control regions B, C and D of the ABCD matrix. This depends on the M_{ℓ^*} parameter; the lowest mass point represents the worst-case scenario where such contamination is maximal, and the highest mass point is the best-case scenario. The effect of the signal leakage in the control regions was estimated for various mass points between $M_{\ell^*} =$ 0.6 and 2.6 TeV, and found to be of the order of 30% in the worst cases. Another source of systematic uncertainties arises from the Z tagging, since there is a discrepancy between the Z tagging efficiency in data and simulation, as discussed in section 4.2.4. Based on the correction factors measured, a 10% uncertainty is assigned the estimated signal efficiency.

7 Final selection and results

Table 6 summarizes the event yield for all channels after applying the selections for the leptons, photon or Z boson, and the invariant mass cuts given in section 4.3. Data agree with the SM expectation and no evidence for new physics is seen.

In the photon channels the main background ($\mathrm{Z}\gamma$) contributes almost 90% of the total. The remaining contributions are $\mathrm{t\bar{t}}\gamma$ ($\lesssim$7%) and jet/ photon misidentification (estimated from data to be $\lesssim$3%), and are rather small in comparison. Similarly in the four lepton channels, about 90% of the backgound arises from ZZ. The jet channels have mixed composition. The main background (Z+Jets) contributes about 50%. The second largest contribution ($\mathrm{t\bar{t}}$) contributes 40% of the expected background. The description of the background is based on the data driven approach described above, but the composition is estimated using simulation, since this information cannot be obtained from the data.

7.1 L-shape search window

After reconstruction of the intermediate boson (photon or Z-boson), two leptons remain to reconstruct the excited lepton, either as $\ell\gamma$ or $\ell\mathrm{Z}$. Thus, both possible lepton+boson invariant masses are calculated, referred to in the following as M^X_{min} and M^X_{max} where X is the channel considered, e^* or μ^*. Figures 4 and 5 show M^X_{min} for all excited electron and muon channels with the background and systematic uncertainties described previously.

JHEP03(2016)125

Channel	N_{bg}	N_{data}	N_{signal} $M_{\ell^*} = 0.6\,\text{TeV}$ $f{=}f'{=}1$ ($f{=}{-}f'{=}1$)		N_{signal} $M_{\ell^*} = 2\,\text{TeV}$ $f{=}f'{=}1$ ($f{=}{-}f'{=}1$)	
			$\Lambda = M_{\ell^*}$	$\Lambda = 4\,\text{TeV}$	$\Lambda = M_{\ell^*}$	$\Lambda = 4\,\text{TeV}$
eeγ	70.4 ± 7.9	62	1.1×10^5 (0)	5.7×10^2 (0)	25 (0)	5.1 (0)
2e2j	22.1 ± 6.0	25	1.3×10^4 (4.6×10^4)	69 (2.4×10^2)	4.7 (16)	1.0 (3.3)
4e	3.0 ± 0.6	0	1.4×10^3 (5.0×10^3)	7.5 (26)	0.3 (1.1)	0.1 (0.2)
2e2μ	2.9 ± 0.5	4	1.8×10^3 (6.2×10^3)	9.3 (32)	0.4 (1.5)	0.1 (0.3)
μμγ	119 ± 15	150	1.2×10^5 (0)	6.4×10^2 (0)	26 (0)	5.4 (0)
2μ2j	20.9 ± 5.6	25	1.6×10^4 (5.6×10^4)	85 (2.9×10^2)	5.9 (20)	1.2 (4.1)
2μ2e	2.5 ± 0.4	2	1.7×10^3 (6.0×10^3)	9.0 (31)	0.4 (1.3)	0.1 (0.3)
4μ	4.0 ± 0.6	4	2.3×10^3 (7.9×10^3)	12.1 (42)	0.5 (1.8)	0.1 (0.4)

Table 6. Expected background events, measured data events and expected signal yields for various channels before the L-shape optimization. Quoted uncertainties are the quadratic sum of statistical and systematic errors. The signal yields are presented for different values of Λ, for the cases $f = f' = 1$ and $f = -f' = 1$. No signal is expected in $\ell\ell^* \to \ell\ell\gamma$ for $f = -f' = 1$.

An illustrative plot of M^X_{min} versus M^X_{max} is given in figure 6. While the expected background tends to be at low invariant masses, a potential signal has the form of an inverted "L" around the excited lepton mass. Defining such a search window discriminates efficiently against background and is referred to in the following as the "final selection" or the "L-shape cut" when defining the final search regions.

The width of these L-shaped search regions depends on the channel and the ℓ^* mass. Detailed values for all channels are given in the appendix. In the muon channels, the mass resolution worsens with increasing energy and the widths of the search windows need to become broader. This can be achieved without affecting the sensitivity of the search, since the high-mass regions are practically background-free. In the electron channels, the improving relative resolution of the electromagnetic calorimeter with increasing energy allows a more precise energy measurement at high masses. As a consequence, the width of the L-shaped windows is chosen individually for the different channels and mass points (by optimizing with respect to the best expected limit). Shown in figure 7 is a comparison of the width of search window with the intrinsic excited lepton width as a function of the

JHEP03(2016)125

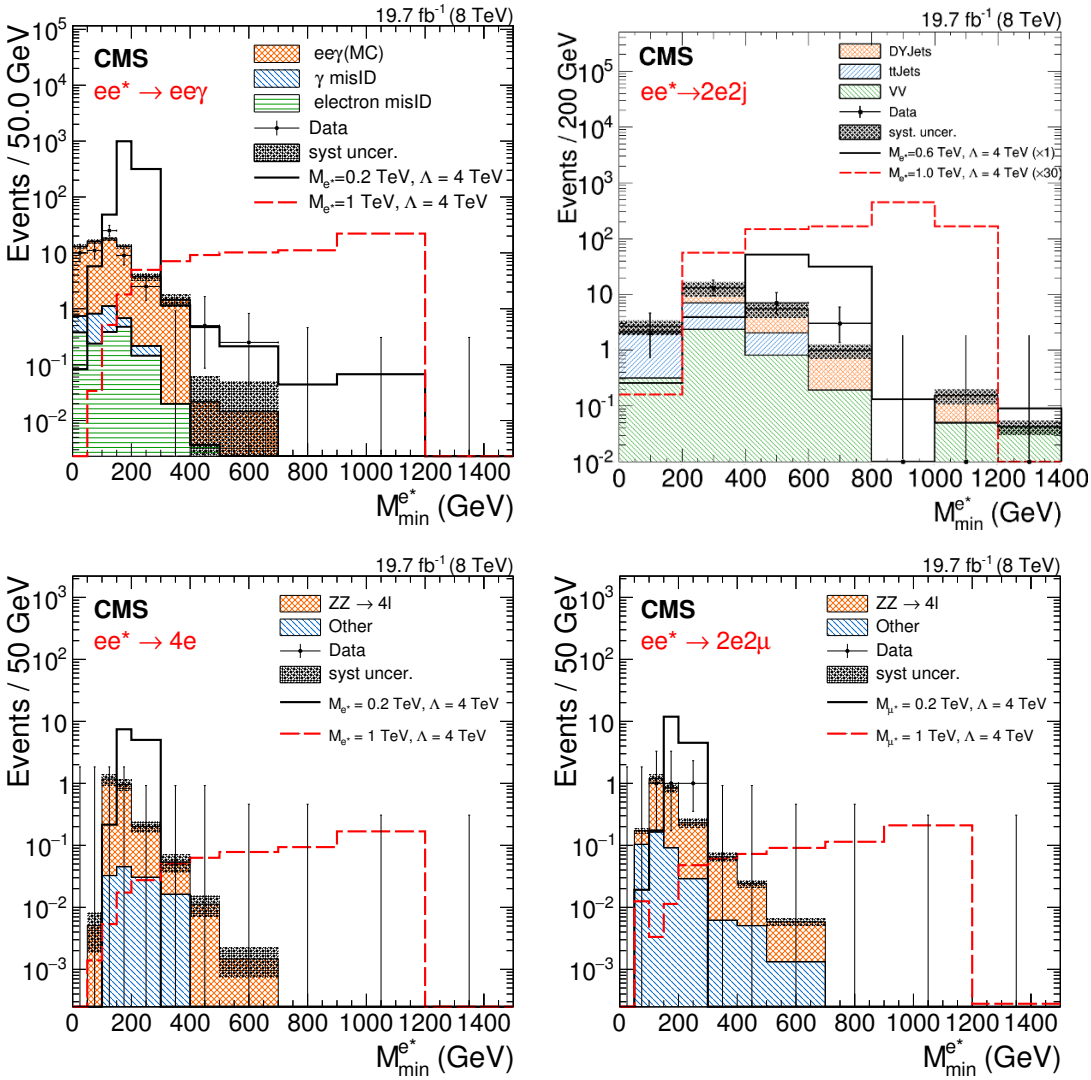

Figure 4. Reconstructed minimum invariant mass from the vector boson (γ, Z) plus one electron for the four excited electron channels. Top left: eeγ, top right: 2e2j, bottom left: 4e, bottom right: 2e2μ. Two signal distributions are shown for $M_{\ell^*} = 0.2$ and 1 TeV, except the 2e2j channel where the trigger threshold only allows searches for $M_{\ell^*} > 0.5$ TeV. The asymmetric error bars indicate the central confidence intervals for Poisson-distributed data and are obtained from the Neyman construction as described in ref. [60].

excited lepton mass, for representative values of the compositeness scale Λ. This figure shows that the mass windows are in general much wider than the intrinsic width of the excited lepton, unless both its mass and Λ are small. The size of the mass window has a negligible effect on the final result, as will be discussed in section 7.2.

The product of acceptance and efficiency as a function of ℓ^* mass for all channels is shown in figure 8. The decreasing efficiency at high masses in the 2ℓ2j channels results from the subjettiness algorithm, which loses ability to resolve the constituents of the fat jets, which overlap more and more with increasing ℓ^* mass.

JHEP03(2016)125

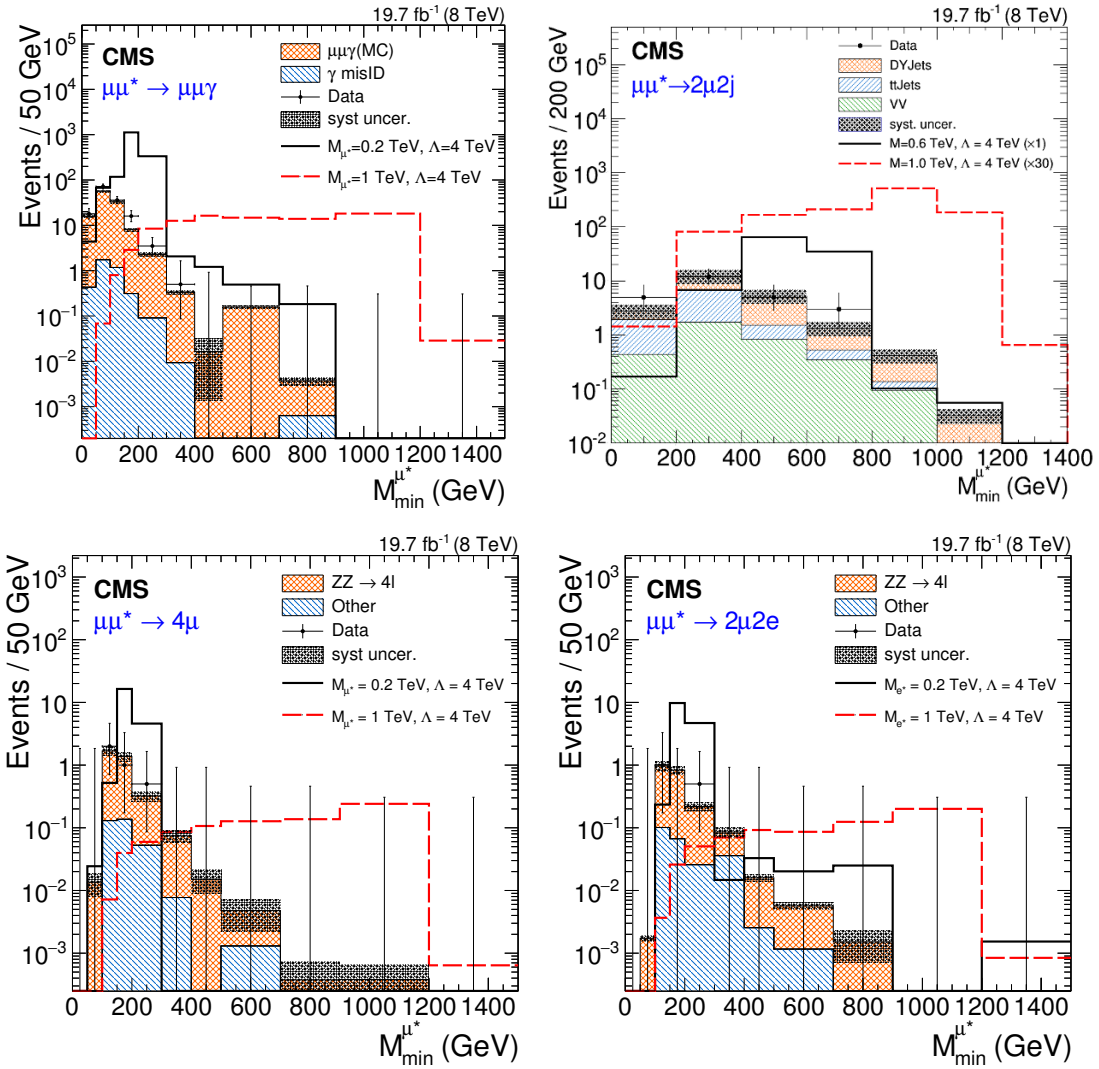

Figure 5. Reconstructed minimum invariant mass from the vector boson (γ, Z) plus one muon for the four excited muon channels. Top left: $\mu\mu\gamma$, top right: $2\mu 2j$, bottom left: 4μ, bottom right: $2\mu 2e$. Two signal distributions are shown for $M_{\ell^*} = 0.2$ and 1 TeV, except the $2\mu 2j$ channel where the trigger threshold only allows searches for $M_{\ell^*} > 0.5$ TeV. The asymmetric error bars indicate the central confidence intervals for Poisson-distributed data and are obtained from the Neyman construction as described in ref. [60].

The selected L-shaped search regions with positions given by the simulated signal masses do not cover the complete M_{min} -M_{max} plane in the low mass region, where the search windows are narrow. To avoid simulating more mass points, those regions are covered with additional L-shaped search regions based on a linear interpolation of the signal expectation between the two closest available simulated signal masses. The 4e channel is used to define the window positions that are adopted in all channels. There, the widths are estimated by linear interpolation between two consecutive masses such that the boundaries of all the search regions are connected. The central positions of these resulting interpolated search windows are then applied in all channels, while the corresponding widths are estimated for each channel individually.

JHEP03(2016)125

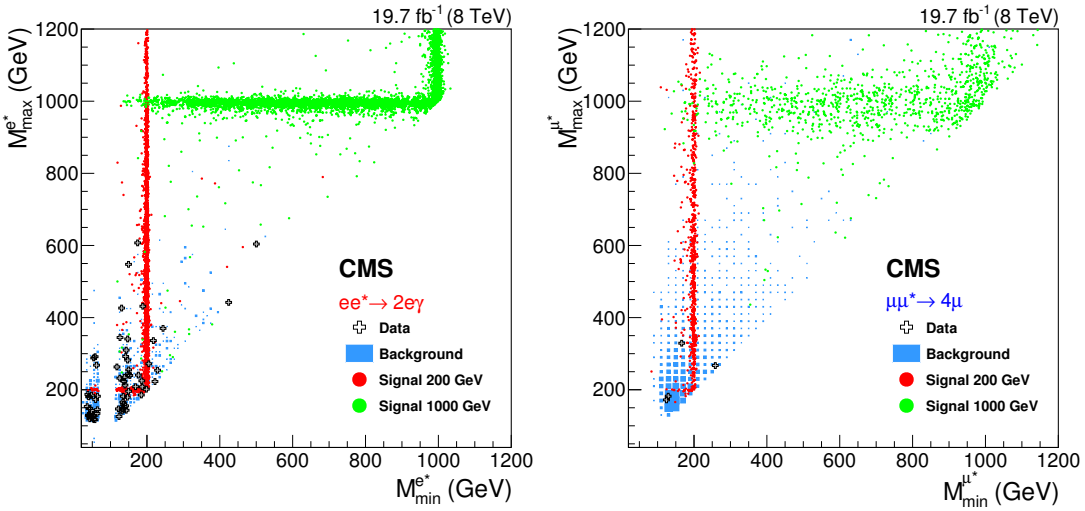

Figure 6. Illustrative two dimensional minimal-versus-maximal invariant-mass distribution for the ee* $\rightarrow$ eeγ (left) and the 4μ channel (right). It can be seen that the resolution worsens with increasing signal mass and that the channels have different resolutions. The left plot clearly shows the effect of the additional Z-veto that is applied in this channel. Background contributions are normalized to the given integrated luminosity, while the normalization of the signal was chosen to enhance visibility.

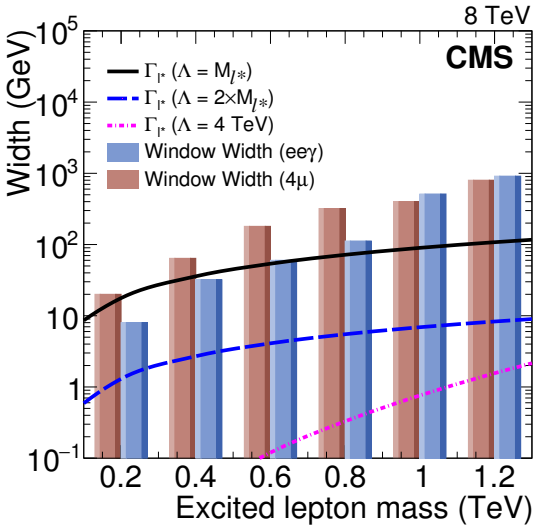

Figure 7. Width of the widest search window (4μ channel) and of a narrow one (eeγ) compared with the intrinsic decay width of the excited lepton, as a function of the ℓ^* mass and for different values of Λ. The latter shows the width of the excited leptons as defined in ref. [7], including GM and CI decays, for the case $f = -f' = 1$.

The observed data, as well as the background expectation, in these newly defined L-shaped search regions are given by the M_{min} -M_{max} distributions. As there are no corresponding signal samples simulated for all these search regions (cf. simulated signal samples as explained in section 2), this information is not available for the signal. The

JHEP03(2016)125

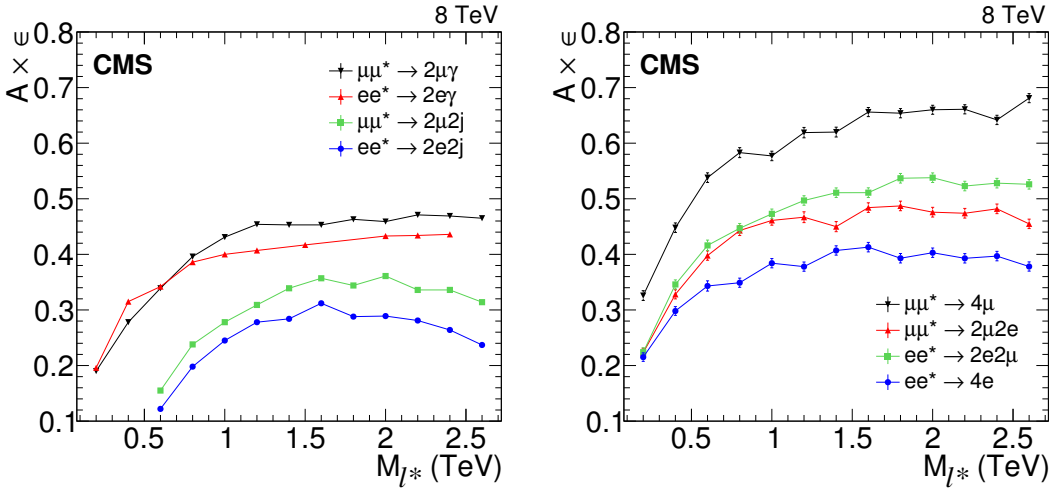

Figure 8. The product of acceptance and efficiency after L-shape selection. In the left panel, the efficiencies for the $\ell\ell^* \to \ell\ell\gamma$ and $2\ell 2j$ channels are shown while the right panel gives the efficiencies of the four-lepton channels. For the $2\ell 2j$ and 4ℓ channels, the values do not include the branching fractions for the specific Z boson decay channel.

signal is therefore estimated by a fit to the signal expectation of the available simulated mass points including the systematic uncertainties.

7.2 Limits on cross section and compositeness scale Λ

The resulting limits of cross section times braching fraction are shown in figure 9. They range from 0.3 fb to 3 fb as a function of M_{ℓ^*}. The four lepton final states: 4e and 2e2μ, 4μ and 2μ2e, differing only in the decay of the SM Z boson, are combined. The other channels are shown individually. The black lines represent the theoretical cross sections including the NLO correction factors for different values of Λ. Solid lines are for the case $f = f' = 1$ while the dashed lines are for $f = -f' = 1$. The 95% confidence level (CL) upper limit on the excited lepton production cross section times branching fraction has been set using a single-bin counting method [61]. The computation has been performed using a Bayesian [62] approach.

The uncertainty bands have interesting behavior in some regions. They become asymmetric and in some cases the 1σ band disappears. Both effects have their origin in the low background expectation in the corresponding search window. In such cases, fluctuations of the limit to lower values are not possible. Unstable behavior of both expected and observed limits is due to the limited number of (background) events in the search regions, with the consequence that the presence of a single event leads to a considerable upward fluctuation of the observed limit (see also tables in the appendix).

The corresponding observed limits on the compositeness scale Λ are displayed in figure 10(left) for the case of SM-like couplings ($f = f' = 1$) and in figure 10(right) for couplings of opposite sign ($f = -f' = 1$). In the latter case, $\ell\ell^* \to \ell\ell\gamma$ cannot contribute. For low M_{ℓ^*} masses compositeness scales up to 16 TeV can be excluded. The sensitivity to Λ decreases with increasing M_{ℓ^*}. For the representative assumption of $M_{\ell^*} = \Lambda$, the

JHEP03(2016)125

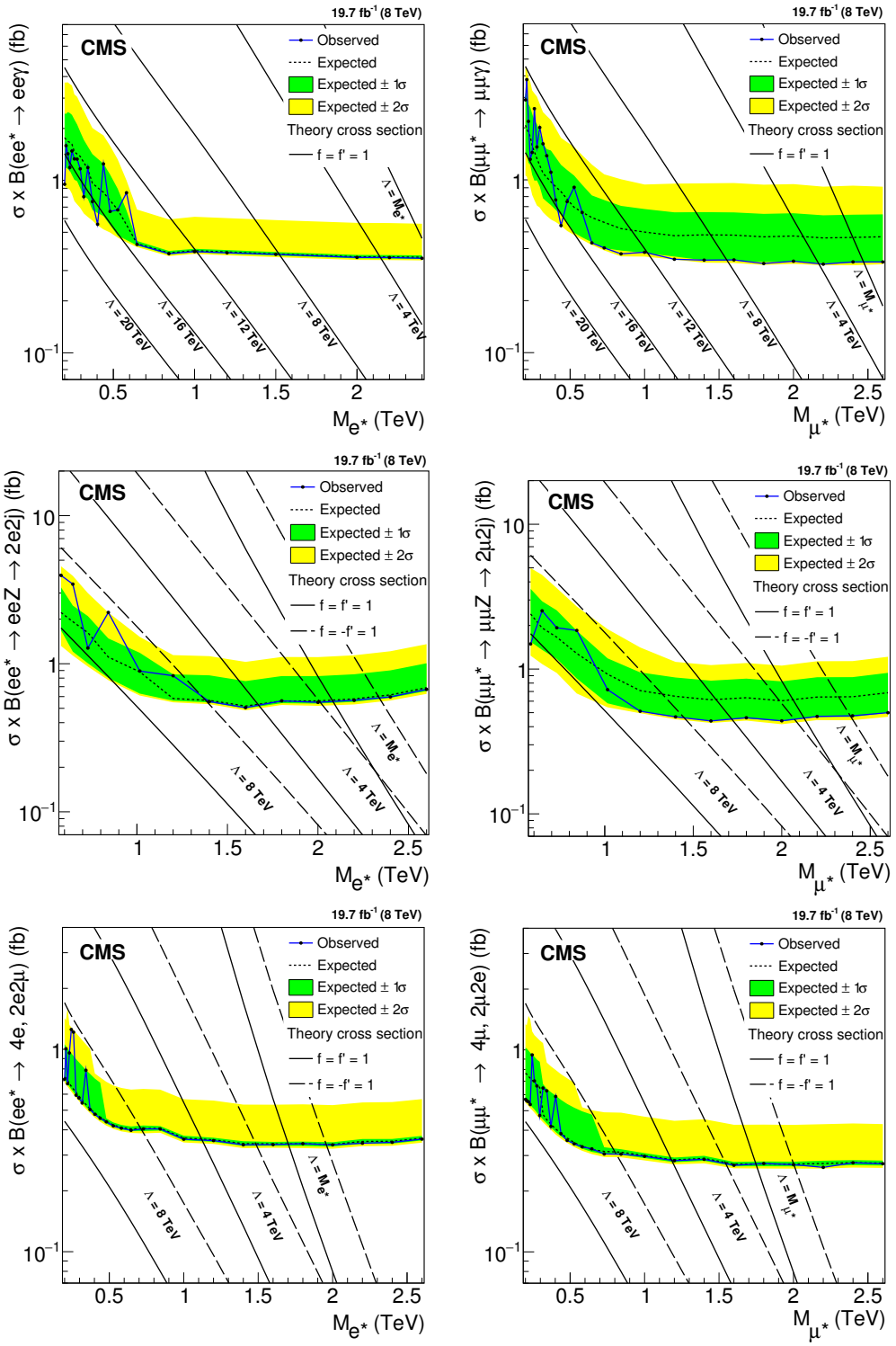

Figure 9. Upper limits at 95% CL on the product of the production cross section and branching fraction for excited electrons (left) and excited muons (right). First row: $\ell\ell^* \to \ell\ell\gamma$, second row: $\ell\ell^* \to \ell\ell Z \to 2\ell 2j$, last row: combined four-lepton results. It is assumed that the signal efficiency is independent of Λ. Theory curves are shown as solid or dashed lines.

JHEP03(2016)125

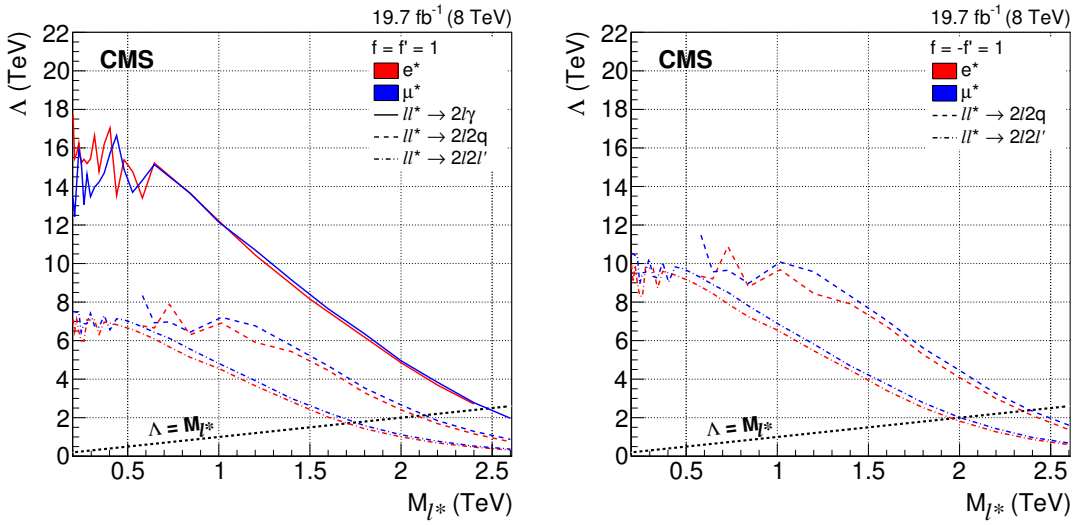

Figure 10. Observed 95% CL limits on the compositeness scale Λ for the cases $f = f' = 1$ and $f = -f' = 1$, as a function of the excited lepton mass for all channels. The excluded values are below the curves.

resulting limits are summarized in table 7 and figure 11. Although, the assumption that the signal efficiency is independent of Λ is not valid for the phase space where Λ and M_{ℓ^*} are small (lower left corner of figures 10), the strong Λ dependence of the cross section, $\sigma \sim 1/\Lambda^4$, leads to a strong increase in sensitivity for low values of Λ and M_{ℓ^*} such that the complete region under the limit curves in figure 10 is nonetheless excluded.

Because of its considerably larger cross section times branching fraction, the $\ell\ell^* \to \ell\ell\gamma$ final state provides the maximum sensitivity for excluding excited leptons with masses up to 2.45 TeV. This limit improves upon the existing ATLAS limit for single ℓ^* production based on a partial 8 TeV data set [20] and exceeds significantly the limits of searches for single excited lepton production at previous colliders. The $\ell\ell^* \to \ell\ell\gamma$ channel shows no sensitivity for the case $f = -f' = 1$, which is therefore studied with Z boson radiation, with the $\ell\ell^* \to \ell\ell\mathrm{Z} \to 2\ell 2\mathrm{j}$ channel being dominant. The excited muon channels are slightly more sensitive than those of the excited electron channels, even though the resolution and thus the signal separation ability of electron final states is higher than that of the muon channels. The higher exclusion power is due to the better muon reconstruction efficiency, which leads to an overall higher signal selection efficiency.

8 Summary

A comprehensive search for excited leptons, e* and μ*, in various channels has been performed using 19.7 fb^{-1} of pp collision data at $\sqrt{s} = 8$ TeV. The excited lepton is assumed to be produced via contact interactions in conjunction with the corresponding standard model lepton. Decaying to its ground state, the excited lepton may emit either a photon or a Z boson. No evidence of excited leptons is found and exclusion limits are set on the compositeness scale Λ as a function of the excited lepton mass M_{ℓ^*}.

The $\ell\ell^* \to \ell\ell\gamma$ final state has the largest production cross section and has therefore previously been used for searches. Following convention, the limits for the assumption

JHEP03(2016)125

Search channel	$M_{\ell^*} = \Lambda$, values in TeV	
	$f = f' = 1$	$f = -f' = 1$
$ee^* \to ee\gamma$	2.45 (2.45)	—
$ee^* \to eeZ \to 2e2j$	2.08 (2.07)	2.34 (2.33)
$ee^* \to eeZ \to 4e$	1.55 (1.55)	1.78 (1.78)
$ee^* \to eeZ \to 2e2\mu$	1.58 (1.58)	1.84 (1.84)
$ee^* \to eeZ \to 2e2\ell$	1.70 (1.70)	1.96 (1.96)
$\mu\mu^* \to \mu\mu\gamma$	2.47 (2.40)	—
$\mu\mu^* \to \mu\mu Z \to 2\mu 2j$	2.11 (2.05)	2.37 (2.31)
$\mu\mu^* \to \mu\mu Z \to 4\mu$	1.64 (1.64)	1.89 (1.89)
$\mu\mu^* \to \mu\mu Z \to 2\mu 2e$	1.58 (1.58)	1.83 (1.83)
$\mu\mu^* \to \mu\mu Z \to 2\mu 2\ell$	1.75 (1.75)	2.00 (2.00)

Table 7. Summary of the observed (expected) limits on ℓ^* mass, assuming $M_{\ell^*} = \Lambda$, for the cases $f = f' = 1$ and $f = -f' = 1$. The latter case is not applicable to $\ell\ell^* \to \ell\ell\gamma$.

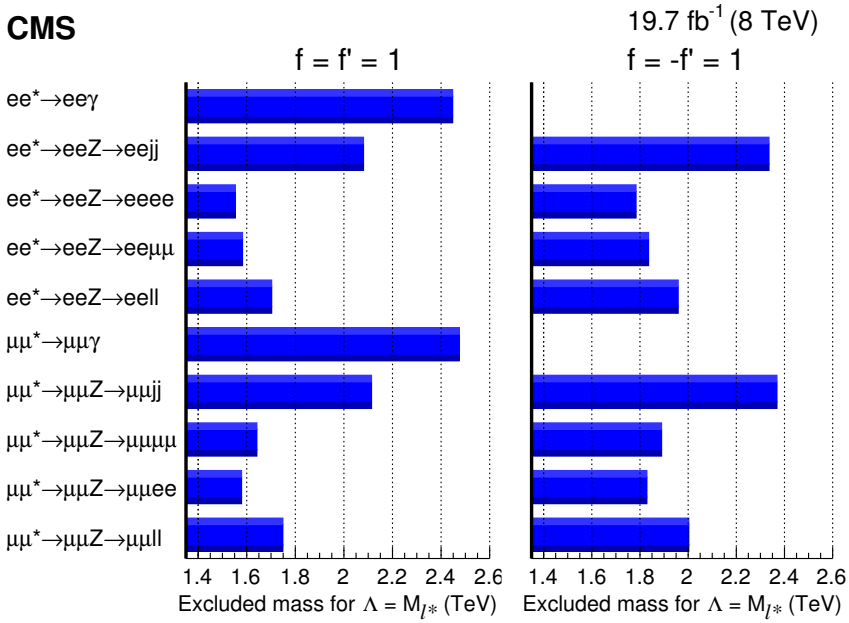

Figure 11. Summary of all mass limits for the various channels and, including the combination of the four lepton channels, for $M_{\ell^*} = \Lambda$.

$\Lambda = M_{\ell^*}$ are included here. This final state yields the best limits, excluding excited electrons up to 2.45 TeV and excited muons up to 2.47 TeV, at 95% confidence level. These limits place the most stringent constraints to date on the existence of excited leptons.

The $\ell^* \to \ell Z$ decay channel has been examined for the first time at hadron colliders, allowing the case where couplings between standard model leptons and excited leptons $f = -f = 1$ can be studied. The leptonic and hadronic (2-jet) final states of the Z boson are used in this search; these final states are Lorentz boosted, requiring a dedicated reconstruction strategy. The observed 95% exclusion limits extend to 2.34 (2.37) TeV for excited electrons (muons), for $f = -f' = 1$.

JHEP03(2016)125

Acknowledgments

We congratulate our colleagues in the CERN accelerator departments for the excellent performance of the LHC and thank the technical and administrative staffs at CERN and at other CMS institutes for their contributions to the success of the CMS effort. In addition, we gratefully acknowledge the computing centres and personnel of the Worldwide LHC Computing Grid for delivering so effectively the computing infrastructure essential to our analyses. Finally, we acknowledge the enduring support for the construction and operation of the LHC and the CMS detector provided by the following funding agencies: the Austrian Federal Ministry of Science, Research and Economy and the Austrian Science Fund; the Belgian Fonds de la Recherche Scientifique, and Fonds voor Wetenschappelijk Onderzoek; the Brazilian Funding Agencies (CNPq, CAPES, FAPERJ, and FAPESP); the Bulgarian Ministry of Education and Science; CERN; the Chinese Academy of Sciences, Ministry of Science and Technology, and National Natural Science Foundation of China; the Colombian Funding Agency (COLCIENCIAS); the Croatian Ministry of Science, Education and Sport, and the Croatian Science Foundation; the Research Promotion Foundation, Cyprus; the Ministry of Education and Research, Estonian Research Council via IUT23-4 and IUT23-6 and European Regional Development Fund, Estonia; the Academy of Finland, Finnish Ministry of Education and Culture, and Helsinki Institute of Physics; the Institut National de Physique Nucléaire et de Physique des Particules / CNRS, and Commissariat à l'Énergie Atomique et aux Énergies Alternatives / CEA, France; the Bundesministerium für Bildung und Forschung, Deutsche Forschungsgemeinschaft, and Helmholtz-Gemeinschaft Deutscher Forschungszentren, Germany; the General Secretariat for Research and Technology, Greece; the National Scientific Research Foundation, and National Innovation Office, Hungary; the Department of Atomic Energy and the Department of Science and Technology, India; the Institute for Studies in Theoretical Physics and Mathematics, Iran; the Science Foundation, Ireland; the Istituto Nazionale di Fisica Nucleare, Italy; the Ministry of Science, ICT and Future Planning, and National Research Foundation (NRF), Republic of Korea; the Lithuanian Academy of Sciences; the Ministry of Education, and University of Malaya (Malaysia); the Mexican Funding Agencies (CINVESTAV, CONACYT, SEP, and UASLP-FAI); the Ministry of Business, Innovation and Employment, New Zealand; the Pakistan Atomic Energy Commission; the Ministry of Science and Higher Education and the National Science Centre, Poland; the Fundação para a Ciência e a Tecnologia, Portugal; JINR, Dubna; the Ministry of Education and Science of the Russian Federation, the Federal Agency of Atomic Energy of the Russian Federation, Russian Academy of Sciences, and the Russian Foundation for Basic Research; the Ministry of Education, Science and Technological Development of Serbia; the Secretaría de Estado de Investigación, Desarrollo e Innovación and Programa Consolider-Ingenio 2010, Spain; the Swiss Funding Agencies (ETH Board, ETH Zurich, PSI, SNF, UniZH, Canton Zurich, and SER); the Ministry of Science and Technology, Taipei; the Thailand Center of Excellence in Physics, the Institute for the Promotion of Teaching Science and Technology of Thailand, Special Task Force for Activating Research and the National Science and Technology Development Agency of Thailand; the Scientific and Technical Research Council of Turkey, and Turkish Atomic Energy Authority; the National Academy of Sciences of Ukraine, and State Fund

JHEP03(2016)125

for Fundamental Researches, Ukraine; the Science and Technology Facilities Council, U.K.; the US Department of Energy, and the US National Science Foundation.

Individuals have received support from the Marie-Curie programme and the European Research Council and EPLANET (European Union); the Leventis Foundation; the A. P. Sloan Foundation; the Alexander von Humboldt Foundation; the Belgian Federal Science Policy Office; the Fonds pour la Formation à la Recherche dans l'Industrie et dans l'Agriculture (FRIA-Belgium); the Agentschap voor Innovatie door Wetenschap en Technologie (IWT-Belgium); the Ministry of Education, Youth and Sports (MEYS) of the Czech Republic; the Council of Science and Industrial Research, India; the HOMING PLUS programme of the Foundation for Polish Science, cofinanced from European Union, Regional Development Fund; the OPUS programme of the National Science Center (Poland); the Compagnia di San Paolo (Torino); the Consorzio per la Fisica (Trieste); MIUR project 20108T4XTM (Italy); the Thalis and Aristeia programmes cofinanced by EU-ESF and the Greek NSRF; the National Priorities Research Program by Qatar National Research Fund; the Rachadapisek Sompot Fund for Postdoctoral Fellowship, Chulalongkorn University (Thailand); and the Welch Foundation, contract C-1845.

A Details of the final selection

Final numbers used to calculate the expected and observed cross section limits for the various excited lepton channels are shown in table 8– 11. In all tables, "window" refers to the interval between the upper and lower invariant mass boundaries of the search windows for the given mass points. The interpolated search windows are not shown. The signal efficiency after all selection steps including the search window is ϵ_{signal}. The expected number of events for the SM background and the number of observed data events are N_{bg} and N_{data}, respectively.

M_{ℓ^*}	$\mu\mu^* \to \mu\mu\gamma$				$ee^* \to ee\gamma$			
(GeV)	Window (GeV)	ϵ_{signal}	N_{bg}	N_{data}	Window (GeV)	ϵ_{signal}	N_{bg}	N_{data}
200	194–206	19.0%	6.95 ± 1.64	10	196–204	19.6%	4.57 ± 1.21	1
400	384–416	27.8%	1.27 ± 0.60	1	384–416	31.5%	1.19 ± 0.61	0
600	564–636	33.9%	0.64 ± 0.48	0	570–630	34.2%	0.40 ± 0.31	2
800	720–880	39.6%	0.29 ± 0.28	0	744–856	38.6%	0.01 ± 0.01	0
1000	720–1280	43.1%	0.29 ± 0.28	0	744–1256	40.0%	0.05 ± 0.04	0
1200	720–1680	45.4%	0.57 ± 0.40	0	744–1656	40.7%	0.05 ± 0.04	0
1400	720–2080	45.3%	0.57 ± 0.40	0	—	—	—	—
1500	—	—	—	—	744–2256	41.7%	0.05 ± 0.04	0
1600	720–2480	45.3%	0.57 ± 0.40	0	—	—	—	—
1800	720–2880	46.3%	0.57 ± 0.40	0	—	—	—	—
2000	720–3280	45.9%	0.57 ± 0.40	0	744–3256	43.3%	0.05 ± 0.04	0
2200	720–3680	47.1%	0.57 ± 0.40	0	744–3656	43.4%	0.05 ± 0.04	0
2400	720–4080	46.9%	0.57 ± 0.40	0	744–4056	43.6%	0.05 ± 0.04	0
2600	720–4480	46.5%	0.57 ± 0.40	0	—	—	—	—

Table 8. Final numbers used to calculate the cross section limits for the excited lepton channels resulting in photon emission, $\mu\mu^* \to \mu\mu\gamma$ and $ee^* \to ee\gamma$.

JHEP03(2016)125

M_{ℓ^*}	$\mu\mu^* \to \mu\mu Z \to 2\mu 2j$				$ee^* \to eeZ \to 2e2j$			
(GeV)	Window (GeV)	ϵ_{signal}	N_{bg}	N_{data}	Window (GeV)	ϵ_{signal}	N_{bg}	N_{data}
600	558–642	15.5%	4.69 ± 1.58	3	570–630	12.2%	3.19 ± 1.11	3
800	728–872	23.8%	3.35 ± 1.15	4	728–856	19.8%	2.49 ± 0.88	3
1000	900–1100	27.8%	1.75 ± 0.63	1	900–1100	24.5%	1.47 ± 0.55	1
1200	1068–1332	30.9%	0.94 ± 0.37	0	1068–1332	27.8%	0.50 ± 0.26	1
1400	1100–1700	33.9%	0.70 ± 0.30	0	1200–1600	28.4%	0.50 ± 0.23	0
1600	1100–2100	35.7%	0.70 ± 0.30	0	1200–2000	31.2%	0.50 ± 0.23	0
1800	1100–2500	34.4%	0.70 ± 0.30	0	1200–2400	28.8%	0.50 ± 0.23	0
2000	1100–2900	36.1%	0.70 ± 0.30	0	1200–2800	28.9%	0.50 ± 0.23	0
2200	1100–3300	33.6%	0.70 ± 0.30	0	1200–3200	28.1%	0.50 ± 0.23	0
2400	1100–3700	33.6%	0.70 ± 0.30	0	1200–3600	26.4%	0.50 ± 0.23	0
2600	1100–4100	31.4%	0.70 ± 0.30	0	1200–4000	23.7%	0.50 ± 0.23	0

Table 9. Final numbers used to calculate the cross section limits for the excited lepton channels resulting in the emission of a Z boson that decays to two jets, $\mu\mu^* \to \mu\mu Z \to 2\mu 2j$ and $ee^* \to eeZ \to 2e2j$.

M_{μ^*}	$\mu\mu^* \to \mu\mu Z \to 4\mu$				$\mu\mu^* \to \mu\mu Z \to 2\mu 2e$			
(GeV)	Window (GeV)	ϵ_{signal}	N_{bg}	N_{data}	Window (GeV)	ϵ_{signal}	N_{bg}	N_{data}
200	190–210	32.6%	0.77 ± 0.12	0	196–204	22.3%	0.23 ± 0.05	0
400	368–432	44.8%	0.23 ± 0.04	0	376–424	32.8%	0.14 ± 0.03	1
600	510–690	53.8%	0.13 ± 0.02	0	540–660	39.8%	0.07 ± 0.03	0
800	640–960	58.3%	0.06 ± 0.01	0	720–880	44.3%	0.04 ± 0.01	0
1000	800–1200	57.7%	0.03 ± 0.01	0	850–1150	46.1%	0.01 ± 0.01	0
1200	800–1600	61.9%	0.04 ± 0.01	0	1000–1400	46.7%	0.00 ± 0.00	0
1400	800–2000	62.0%	0.04 ± 0.01	0	1200–1800	45.0%	0.01 ± 0.01	0
1600	800–2400	65.6%	0.04 ± 0.01	0	1200–2200	48.4%	0.01 ± 0.01	0
1800	800–2800	65.4%	0.04 ± 0.01	0	1200–2600	48.7%	0.01 ± 0.01	0
2000	800–3200	66.0%	0.04 ± 0.01	0	1200–3000	47.6%	0.01 ± 0.01	0
2200	800–3600	66.1%	0.04 ± 0.01	0	1200–3400	47.4%	0.01 ± 0.01	0
2400	800–4000	64.2%	0.04 ± 0.01	0	1200–3800	48.2%	0.01 ± 0.01	0
2600	800–4400	68.1%	0.04 ± 0.01	0	1200–4200	45.5%	0.01 ± 0.01	0

Table 10. Final numbers used to calculate the cross section limits for the two excited muon channels in the 4ℓ final states.

JHEP03(2016)125

M_{e^*}	$ee^* \to eeZ \to 4e$				$ee^* \to eeZ \to 2e2\mu$			
(GeV)	Window (GeV)	ϵ_{signal}	N_{bg}	N_{data}	Window (GeV)	ϵ_{signal}	N_{bg}	N_{data}
200	196–204	21.5%	0.23 ± 0.05	0	196–204	22.4%	0.24 ± 0.05	0
400	384–416	29.8%	0.08 ± 0.02	0	384–416	34.6%	0.09 ± 0.02	0
600	570–630	34.3%	0.03 ± 0.01	0	552–648	41.6%	0.08 ± 0.02	0
800	744–856	34.9%	0.01 ± 0.00	0	728–872	44.7%	0.02 ± 0.01	0
1000	900–1100	38.4%	0.01 ± 0.00	0	860–1140	47.3%	0.02 ± 0.01	0
1200	1000–1200	37.8%	0.01 ± 0.01	0	860–1540	49.7%	0.02 ± 0.01	0
1400	1000–1600	40.7%	0.01 ± 0.01	0	860–1940	51.1%	0.02 ± 0.01	0
1600	1000–2000	41.3%	0.01 ± 0.01	0	860–2340	51.1%	0.02 ± 0.01	0
1800	1000–2400	39.3%	0.01 ± 0.01	0	860–2740	53.7%	0.02 ± 0.01	0
2000	1000–2800	40.3%	0.01 ± 0.01	0	860–3140	53.8%	0.02 ± 0.01	0
2200	1000–3200	39.3%	0.01 ± 0.01	0	860–3540	52.3%	0.02 ± 0.01	0
2400	1000–3800	39.7%	0.01 ± 0.01	0	860–3940	52.8%	0.02 ± 0.01	0
2600	1000–4200	37.8%	0.01 ± 0.01	0	860–4340	52.6%	0.02 ± 0.01	0

Table 11. Final numbers used to calculate the cross section limits for the two excited electron channels in the 4ℓ final states.

References

[1] J.C. Pati, A. Salam and J.A. Strathdee, *Are quarks composite?*, *Phys. Lett.* **B 59** (1975) 265 [INSPIRE].

[2] H. Terazawa, M. Yasuè, K. Akama and M. Hayashi, *Observable effects of the possible substructure of leptons and quarks*, *Phys. Lett.* **B 112** (1982) 387 [INSPIRE].

[3] M. Abolins et al., *Testing the compositeness of quarks and leptons*, *eConf* **C 8206282** (1982) 274 [INSPIRE].

[4] E. Eichten, K.D. Lane and M.E. Peskin, *New tests for quark and lepton substructure*, *Phys. Rev. Lett.* **50** (1983) 811 [INSPIRE].

[5] H. Harari, *Composite models for quarks and leptons*, *Phys. Rept.* **104** (1984) 159.

[6] K.D. Lane, F.E. Paige, T. Skwarnicki and W.J. Womersley, *Simulations of supercollider physics*, *Phys. Rept.* **278** (1997) 291 [hep-ph/9412280] [INSPIRE].

[7] U. Baur, M. Spira and P.M. Zerwas, *Excited quark and lepton production at hadron colliders*, *Phys. Rev.* **D 42** (1990) 815 [INSPIRE].

[8] O.W. Greenberg and C.A. Nelson, *Composite models of leptons*, *Phys. Rev.* **D 10** (1974) 2567 [INSPIRE].

[9] O.W. Greenberg and J. Sucher, *A quantum structure dynamic model of quarks, leptons, weak vector bosons and Higgs mesons*, *Phys. Lett.* **B 99** (1981) 339 [INSPIRE].

JHEP03(2016)125

[10] ALEPH collaboration, D. Buskulic et al., *Search for excited leptons at* 130 *GeV*–140 *GeV*, *Phys. Lett.* **B 385** (1996) 445 [INSPIRE].

[11] DELPHI collaboration, P. Abreu et al., *Search for composite and exotic fermions at LEP-2*, *Eur. Phys. J.* **C 8** (1999) 41 [hep-ex/9811005] [INSPIRE].

[12] OPAL collaboration, G. Abbiendi et al., *Search for unstable heavy and excited leptons at LEP-2*, *Eur. Phys. J.* **C 14** (2000) 73 [hep-ex/0001056] [INSPIRE].

[13] L3 collaboration, P. Achard et al., *Search for excited leptons at LEP*, *Phys. Lett.* **B 568** (2003) 23 [hep-ex/0306016] [INSPIRE].

[14] H1 collaboration, F.D. Aaron et al., *Search for excited electrons in ep collisions at HERA*, *Phys. Lett.* **B 666** (2008) 131 [arXiv:0805.4530] [INSPIRE].

[15] CDF collaboration, D. Acosta et al., *Search for excited and exotic electrons in the $e\gamma$ decay channel in $p\bar{p}$ collisions at $\sqrt{s} = 1.96$ TeV*, *Phys. Rev. Lett.* **94** (2005) 101802 [hep-ex/0410013] [INSPIRE].

[16] CDF collaboration, A. Abulencia et al., *Search for excited and exotic muons in the $\mu\gamma$ decay channel in $p\bar{p}$ collisions at $\sqrt{s} = 1.96$ TeV*, *Phys. Rev. Lett.* **97** (2006) 191802 [hep-ex/0606043] [INSPIRE].

[17] D0 collaboration, V.M. Abazov et al., *Search for excited muons in $p\bar{p}$ collisions at $\sqrt{s} = 1.96$ TeV*, *Phys. Rev.* **D 73** (2006) 111102 [hep-ex/0604040] [INSPIRE].

[18] D0 collaboration, V.M. Abazov et al., *Search for excited electrons in $p\bar{p}$ collisions at $\sqrt{s} = 1.96$ TeV*, *Phys. Rev.* **D 77** (2008) 091102 [arXiv:0801.0877] [INSPIRE].

[19] CMS collaboration, *Search for excited leptons in pp collisions at $\sqrt{s} = 7$ TeV*, *Phys. Lett.* **B 720** (2013) 309 [arXiv:1210.2422] [INSPIRE].

[20] ATLAS collaboration, *Search for excited electrons and muons in $\sqrt{s} = 8$ TeV proton-proton collisions with the ATLAS detector*, *New J. Phys.* **15** (2013) 093011 [arXiv:1308.1364] [INSPIRE].

[21] CMS collaboration, *CMS luminosity based on pixel cluster counting — Summer 2013 update*, CMS-PAS-LUM-13-001 (2013).

[22] T. Sjöstrand, S. Mrenna and P.Z. Skands, *A brief introduction to PYTHIA 8.1*, *Comput. Phys. Commun.* **178** (2008) 852 [arXiv:0710.3820] [INSPIRE].

[23] T. Sjöstrand, S. Mrenna and P.Z. Skands, *PYTHIA 6.4 physics and manual*, *JHEP* **05** (2006) 026 [hep-ph/0603175] [INSPIRE].

[24] GEANT4 collaboration, S. Agostinelli et al., *GEANT4 — A simulation toolkit*, *Nucl. Instrum. Meth.* **A 506** (2003) 250 [INSPIRE].

[25] J. Pumplin, D.R. Stump, J. Huston, H.L. Lai, P.M. Nadolsky and W.K. Tung, *New generation of parton distributions with uncertainties from global QCD analysis*, *JHEP* **07** (2002) 012 [hep-ph/0201195] [INSPIRE].

[26] S. Majhi, *QCD corrections to excited lepton (pair) production at the LHC*, *Phys. Rev.* **D 88** (2013) 074028 [arXiv:1210.8307] [INSPIRE].

[27] CMS collaboration, *The CMS experiment at the CERN LHC*, 2008 *JINST* **3** S08004.

[28] CMS collaboration, *Performance of photon reconstruction and identification with the CMS detector in proton-proton collisions at $\sqrt{s} = 8$ TeV*, 2015 *JINST* **10** P08010 [arXiv:1502.02702] [INSPIRE].

JHEP03(2016)125

[29] CMS collaboration, *Performance of electron reconstruction and selection with the CMS detector in proton-proton collisions at* $\sqrt{s} = 8$ *TeV*, 2015 *JINST* **10** P06005 [arXiv:1502.02701] [INSPIRE].

[30] CMS collaboration, *Performance of CMS muon reconstruction in pp collision events at* $\sqrt{s} = 7$ *TeV*, 2012 *JINST* **7** P10002 [arXiv:1206.4071] [INSPIRE].

[31] CMS collaboration, *Search for heavy narrow dilepton resonances in pp collisions at* $\sqrt{s} = 7$ *TeV and* $\sqrt{s} = 8$ *TeV*, *Phys. Lett.* **B 720** (2013) 63 [arXiv:1212.6175] [INSPIRE].

[32] M. Cacciari, G.P. Salam and G. Soyez, *FastJet user manual*, *Eur. Phys. J.* **C 72** (2012) 1896 [arXiv:1111.6097] [INSPIRE].

[33] CMS collaboration, *Search for massive resonances decaying into pairs of boosted bosons in semi-leptonic final states at* $\sqrt{s} = 8$ *TeV*, *JHEP* **08** (2014) 174 [arXiv:1405.3447] [INSPIRE].

[34] CMS collaboration, *Commissioning of the particle-flow event reconstruction with the first LHC collisions recorded in the CMS detector*, CMS-PAS-PFT-10-001 (2010).

[35] M. Wobisch and T. Wengler, *Hadronization corrections to jet cross-sections in deep inelastic scattering*, in the proceedings of the *Workshop on Monte Carlo Generators for HERA Physics* (1998), hep-ph/9907280 [INSPIRE].

[36] CMS collaboration, *Determination of jet energy calibration and transverse momentum resolution in CMS*, 2011 *JINST* **6** P11002 [arXiv:1107.4277] [INSPIRE].

[37] S.D. Ellis, C.K. Vermilion and J.R. Walsh, *Techniques for improved heavy particle searches with jet substructure*, *Phys. Rev.* **D 80** (2009) 051501 [arXiv:0903.5081] [INSPIRE].

[38] S.D. Ellis, C.K. Vermilion and J.R. Walsh, *Recombination algorithms and jet substructure: pruning as a tool for heavy particle searches*, *Phys. Rev.* **D 81** (2010) 094023 [arXiv:0912.0033] [INSPIRE].

[39] CMS collaboration, *Search for anomalous* $t\bar{t}$ *production in the highly-boosted all-hadronic final state*, *JHEP* **09** (2012) 029 [*Erratum ibid.* **03** (2014) 132] [arXiv:1204.2488] [INSPIRE].

[40] CMS collaboration, *Studies of jet mass in dijet and* W/Z *+ jet events*, *JHEP* **05** (2013) 090 [arXiv:1303.4811] [INSPIRE].

[41] CMS collaboration, *Search for heavy resonances in the* W/Z*-tagged dijet mass spectrum in pp collisions at* 7 *TeV*, *Phys. Lett.* **B 723** (2013) 280 [arXiv:1212.1910] [INSPIRE].

[42] CMS collaboration, *Identification techniques for highly boosted W bosons that decay into hadrons*, *JHEP* **12** (2014) 017 [arXiv:1410.4227] [INSPIRE].

[43] J. Thaler and K. Van Tilburg, *Identifying boosted objects with* N*-subjettiness*, *JHEP* **03** (2011) 015 [arXiv:1011.2268] [INSPIRE].

[44] J. Thaler and K. Van Tilburg, *Maximizing boosted top identification by minimizing* N*-subjettiness*, *JHEP* **02** (2012) 093 [arXiv:1108.2701] [INSPIRE].

[45] I.W. Stewart, F.J. Tackmann and W.J. Waalewijn, N*-jettiness: an inclusive event shape to veto jets*, *Phys. Rev. Lett.* **105** (2010) 092002 [arXiv:1004.2489] [INSPIRE].

[46] S. Catani, Y.L. Dokshitzer, M.H. Seymour and B.R. Webber, *Longitudinally invariant* K_t *clustering algorithms for hadron hadron collisions*, *Nucl. Phys.* **B 406** (1993) 187 [INSPIRE].

[47] S.D. Ellis and D.E. Soper, *Successive combination jet algorithm for hadron collisions*, *Phys. Rev.* **D 48** (1993) 3160 [hep-ph/9305266] [INSPIRE].

JHEP03(2016)125

[48] T. Gleisberg et al., *Event generation with SHERPA 1.1*, *JHEP* **02** (2009) 007 [arXiv:0811.4622] [INSPIRE].

[49] J.M. Campbell, R.K. Ellis and D.L. Rainwater, *Next-to-leading order QCD predictions for $W+2$ jet and $Z+2$ jet production at the CERN LHC*, *Phys. Rev.* **D 68** (2003) 094021 [hep-ph/0308195] [INSPIRE].

[50] J.M. Campbell, R.K. Ellis and C. Williams, *Vector boson pair production at the LHC*, *JHEP* **07** (2011) 018 [arXiv:1105.0020] [INSPIRE].

[51] J. Alwall, M. Herquet, F. Maltoni, O. Mattelaer and T. Stelzer, *MadGraph 5: going beyond*, *JHEP* **06** (2011) 128 [arXiv:1106.0522] [INSPIRE].

[52] T. Binoth, N. Kauer and P. Mertsch, *Gluon-induced QCD corrections to $pp \to ZZ \to l\bar{l}l'\bar{l}'$*, talk given at the *Deep Inelastic Scattering Workshop (DIS 2008)*, April 7–11, London, U.K. (2008), arXiv:0807.0024 [INSPIRE].

[53] P. Nason, *A new method for combining NLO QCD with shower Monte Carlo algorithms*, *JHEP* **11** (2004) 040 [hep-ph/0409146] [INSPIRE].

[54] S. Frixione, P. Nason and C. Oleari, *Matching NLO QCD computations with parton shower simulations: the POWHEG method*, *JHEP* **11** (2007) 070 [arXiv:0709.2092] [INSPIRE].

[55] S. Alioli, P. Nason, C. Oleari and E. Re, *A general framework for implementing NLO calculations in shower Monte Carlo programs: the POWHEG BOX*, *JHEP* **06** (2010) 043 [arXiv:1002.2581] [INSPIRE].

[56] T. Melia, P. Nason, R. Rontsch and G. Zanderighi, *W^+W^-, WZ and ZZ production in the POWHEG BOX*, *JHEP* **11** (2011) 078 [arXiv:1107.5051] [INSPIRE].

[57] CMS collaboration, *Measurement of the $pp \to ZZ$ production cross section and constraints on anomalous triple gauge couplings in four-lepton final states at $\sqrt{s} = 8$ TeV*, *Phys. Lett.* **B 740** (2015) 250 [arXiv:1406.0113] [INSPIRE].

[58] S. Alekhin et al., *The PDF4LHC working group interim report*, arXiv:1101.0536 [INSPIRE].

[59] M. Botje et al., *The PDF4LHC working group interim recommendations*, arXiv:1101.0538 [INSPIRE].

[60] F. Garwood, *Fiducial limits for the Poisson distribution*, *Biometrika* **28** (1936) 437.

[61] ATLAS and CMS and The LHC Higgs Combination Group, *Procedure for the LHC Higgs boson search combination in Summer 2011*, CMS-NOTE-2011-005 (2011).

[62] J. Heinrich et al., *Interval estimation in the presence of nuisance parameters. 1. Bayesian approach*, physics/0409129 [INSPIRE].

JHEP03(2016)125

The CMS collaboration

Yerevan Physics Institute, Yerevan, Armenia

V. Khachatryan, A.M. Sirunyan, A. Tumasyan

Institut für Hochenergiephysik der OeAW, Wien, Austria

W. Adam, E. Asilar, T. Bergauer, J. Brandstetter, E. Brondolin, M. Dragicevic, J. Erö, M. Flechl, M. Friedl, R. Frühwirth[1], V.M. Ghete, C. Hartl, N. Hörmann, J. Hrubec, M. Jeitler[1], V. Knünz, A. König, M. Krammer[1], I. Krätschmer, D. Liko, T. Matsushita, I. Mikulec, D. Rabady[2], B. Rahbaran, H. Rohringer, J. Schieck[1], R. Schöfbeck, J. Strauss, W. Treberer-Treberspurg, W. Waltenberger, C.-E. Wulz[1]

National Centre for Particle and High Energy Physics, Minsk, Belarus

V. Mossolov, N. Shumeiko, J. Suarez Gonzalez

Universiteit Antwerpen, Antwerpen, Belgium

S. Alderweireldt, T. Cornelis, E.A. De Wolf, X. Janssen, A. Knutsson, J. Lauwers, S. Luyckx, R. Rougny, M. Van De Klundert, H. Van Haevermaet, P. Van Mechelen, N. Van Remortel, A. Van Spilbeeck

Vrije Universiteit Brussel, Brussel, Belgium

S. Abu Zeid, F. Blekman, J. D'Hondt, N. Daci, I. De Bruyn, K. Deroover, N. Heracleous, J. Keaveney, S. Lowette, L. Moreels, A. Olbrechts, Q. Python, D. Strom, S. Tavernier, W. Van Doninck, P. Van Mulders, G.P. Van Onsem, I. Van Parijs

Université Libre de Bruxelles, Bruxelles, Belgium

P. Barria, H. Brun, C. Caillol, B. Clerbaux, G. De Lentdecker, G. Fasanella, L. Favart, A. Grebenyuk, G. Karapostoli, T. Lenzi, A. Léonard, T. Maerschalk, A. Marinov, L. Perniè, A. Randle-conde, T. Reis, T. Seva, C. Vander Velde, P. Vanlaer, R. Yonamine, F. Zenoni, F. Zhang[3]

Ghent University, Ghent, Belgium

K. Beernaert, L. Benucci, A. Cimmino, S. Crucy, D. Dobur, A. Fagot, G. Garcia, M. Gul, J. Mccartin, A.A. Ocampo Rios, D. Poyraz, D. Ryckbosch, S. Salva, M. Sigamani, N. Strobbe, M. Tytgat, W. Van Driessche, E. Yazgan, N. Zaganidis

Université Catholique de Louvain, Louvain-la-Neuve, Belgium

S. Basegmez, C. Beluffi[4], O. Bondu, S. Brochet, G. Bruno, A. Caudron, L. Ceard, G.G. Da Silveira, C. Delaere, D. Favart, L. Forthomme, A. Giammanco[5], J. Hollar, A. Jafari, P. Jez, M. Komm, V. Lemaitre, A. Mertens, C. Nuttens, L. Perrini, A. Pin, K. Piotrzkowski, A. Popov[6], L. Quertenmont, M. Selvaggi, M. Vidal Marono

Université de Mons, Mons, Belgium

N. Beliy, G.H. Hammad

Centro Brasileiro de Pesquisas Fisicas, Rio de Janeiro, Brazil

W.L. Aldá Júnior, G.A. Alves, L. Brito, M. Correa Martins Junior, M. Hamer, C. Hensel, C. Mora Herrera, A. Moraes, M.E. Pol, P. Rebello Teles

JHEP03(2016)125

Universidade do Estado do Rio de Janeiro, Rio de Janeiro, Brazil

E. Belchior Batista Das Chagas, W. Carvalho, J. Chinellato[7], A. Custódio, E.M. Da Costa, D. De Jesus Damiao, C. De Oliveira Martins, S. Fonseca De Souza, L.M. Huertas Guativa, H. Malbouisson, D. Matos Figueiredo, L. Mundim, H. Nogima, W.L. Prado Da Silva, A. Santoro, A. Sznajder, E.J. Tonelli Manganote[7], A. Vilela Pereira

Universidade Estadual Paulista [a], Universidade Federal do ABC [b], São Paulo, Brazil

S. Ahuja[a], C.A. Bernardes[b], A. De Souza Santos[b], S. Dogra[a], T.R. Fernandez Perez Tomei[a], E.M. Gregores[b], P.G. Mercadante[b], C.S. Moon[a,8], S.F. Novaes[a], Sandra S. Padula[a], D. Romero Abad, J.C. Ruiz Vargas

Institute for Nuclear Research and Nuclear Energy, Sofia, Bulgaria

A. Aleksandrov, R. Hadjiiska, P. Iaydjiev, M. Rodozov, S. Stoykova, G. Sultanov, M. Vutova

University of Sofia, Sofia, Bulgaria

A. Dimitrov, I. Glushkov, L. Litov, B. Pavlov, P. Petkov

Institute of High Energy Physics, Beijing, China

M. Ahmad, J.G. Bian, G.M. Chen, H.S. Chen, M. Chen, T. Cheng, R. Du, C.H. Jiang, R. Plestina[9], F. Romeo, S.M. Shaheen, J. Tao, C. Wang, Z. Wang, H. Zhang

State Key Laboratory of Nuclear Physics and Technology, Peking University, Beijing, China

C. Asawatangtrakuldee, Y. Ban, Q. Li, S. Liu, Y. Mao, S.J. Qian, D. Wang, Z. Xu

Universidad de Los Andes, Bogota, Colombia

C. Avila, A. Cabrera, L.F. Chaparro Sierra, C. Florez, J.P. Gomez, B. Gomez Moreno, J.C. Sanabria

University of Split, Faculty of Electrical Engineering, Mechanical Engineering and Naval Architecture, Split, Croatia

N. Godinovic, D. Lelas, I. Puljak, P.M. Ribeiro Cipriano

University of Split, Faculty of Science, Split, Croatia

Z. Antunovic, M. Kovac

Institute Rudjer Boskovic, Zagreb, Croatia

V. Brigljevic, K. Kadija, J. Luetic, S. Micanovic, L. Sudic

University of Cyprus, Nicosia, Cyprus

A. Attikis, G. Mavromanolakis, J. Mousa, C. Nicolaou, F. Ptochos, P.A. Razis, H. Rykaczewski

Charles University, Prague, Czech Republic

M. Bodlak, M. Finger[10], M. Finger Jr.[10]

JHEP03(2016)125

Academy of Scientific Research and Technology of the Arab Republic of Egypt, Egyptian Network of High Energy Physics, Cairo, Egypt
Y. Assran[11], S. Elgammal[12], A. Ellithi Kamel[13,13], M.A. Mahmoud[14,14]

National Institute of Chemical Physics and Biophysics, Tallinn, Estonia
B. Calpas, M. Kadastik, M. Murumaa, M. Raidal, A. Tiko, C. Veelken

Department of Physics, University of Helsinki, Helsinki, Finland
P. Eerola, J. Pekkanen, M. Voutilainen

Helsinki Institute of Physics, Helsinki, Finland
J. Härkönen, V. Karimäki, R. Kinnunen, T. Lampén, K. Lassila-Perini, S. Lehti, T. Lindén, P. Luukka, T. Mäenpää, T. Peltola, E. Tuominen, J. Tuominiemi, E. Tuovinen, L. Wendland

Lappeenranta University of Technology, Lappeenranta, Finland
J. Talvitie, T. Tuuva

DSM/IRFU, CEA/Saclay, Gif-sur-Yvette, France
M. Besancon, F. Couderc, M. Dejardin, D. Denegri, B. Fabbro, J.L. Faure, C. Favaro, F. Ferri, S. Ganjour, A. Givernaud, P. Gras, G. Hamel de Monchenault, P. Jarry, E. Locci, M. Machet, J. Malcles, J. Rander, A. Rosowsky, M. Titov, A. Zghiche

Laboratoire Leprince-Ringuet, Ecole Polytechnique, IN2P3-CNRS, Palaiseau, France
I. Antropov, S. Baffioni, F. Beaudette, P. Busson, L. Cadamuro, E. Chapon, C. Charlot, T. Dahms, O. Davignon, N. Filipovic, A. Florent, R. Granier de Cassagnac, S. Lisniak, L. Mastrolorenzo, P. Miné, I.N. Naranjo, M. Nguyen, C. Ochando, G. Ortona, P. Paganini, P. Pigard, S. Regnard, R. Salerno, J.B. Sauvan, Y. Sirois, T. Strebler, Y. Yilmaz, A. Zabi

Institut Pluridisciplinaire Hubert Curien, Université de Strasbourg, Université de Haute Alsace Mulhouse, CNRS/IN2P3, Strasbourg, France
J.-L. Agram[15], J. Andrea, A. Aubin, D. Bloch, J.-M. Brom, M. Buttignol, E.C. Chabert, N. Chanon, C. Collard, E. Conte[15], X. Coubez, J.-C. Fontaine[15], D. Gelé, U. Goerlach, C. Goetzmann, A.-C. Le Bihan, J.A. Merlin[2], K. Skovpen, P. Van Hove

Centre de Calcul de l'Institut National de Physique Nucleaire et de Physique des Particules, CNRS/IN2P3, Villeurbanne, France
S. Gadrat

Université de Lyon, Université Claude Bernard Lyon 1, CNRS-IN2P3, Institut de Physique Nucléaire de Lyon, Villeurbanne, France
S. Beauceron, C. Bernet, G. Boudoul, E. Bouvier, C.A. Carrillo Montoya, R. Chierici, D. Contardo, B. Courbon, P. Depasse, H. El Mamouni, J. Fan, J. Fay, S. Gascon, M. Gouzevitch, B. Ille, F. Lagarde, I.B. Laktineh, M. Lethuillier, L. Mirabito, A.L. Pequegnot, S. Perries, J.D. Ruiz Alvarez, D. Sabes, L. Sgandurra, V. Sordini, M. Vander Donckt, P. Verdier, S. Viret

JHEP03(2016)125

Georgian Technical University, Tbilisi, Georgia
T. Toriashvili[16]

Tbilisi State University, Tbilisi, Georgia
I. Bagaturia[17]

RWTH Aachen University, I. Physikalisches Institut, Aachen, Germany
C. Autermann, S. Beranek, M. Edelhoff, L. Feld, A. Heister, M.K. Kiesel, K. Klein, M. Lipinski, A. Ostapchuk, M. Preuten, F. Raupach, S. Schael, J.F. Schulte, T. Verlage, H. Weber, B. Wittmer, V. Zhukov[6]

RWTH Aachen University, III. Physikalisches Institut A, Aachen, Germany
M. Ata, M. Brodski, E. Dietz-Laursonn, D. Duchardt, M. Endres, M. Erdmann, S. Erdweg, T. Esch, R. Fischer, A. Güth, T. Hebbeker, C. Heidemann, K. Hoepfner, D. Klingebiel, S. Knutzen, P. Kreuzer, M. Merschmeyer, A. Meyer, P. Millet, M. Olschewski, K. Padeken, P. Papacz, T. Pook, M. Radziej, H. Reithler, M. Rieger, F. Scheuch, L. Sonnenschein, D. Teyssier, S. Thüer

RWTH Aachen University, III. Physikalisches Institut B, Aachen, Germany
V. Cherepanov, Y. Erdogan, G. Flügge, H. Geenen, M. Geisler, F. Hoehle, B. Kargoll, T. Kress, Y. Kuessel, A. Künsken, J. Lingemann[2], A. Nehrkorn, A. Nowack, I.M. Nugent, C. Pistone, O. Pooth, A. Stahl

Deutsches Elektronen-Synchrotron, Hamburg, Germany
M. Aldaya Martin, I. Asin, N. Bartosik, O. Behnke, U. Behrens, A.J. Bell, K. Borras, A. Burgmeier, A. Cakir, L. Calligaris, A. Campbell, S. Choudhury, F. Costanza, C. Diez Pardos, G. Dolinska, S. Dooling, T. Dorland, G. Eckerlin, D. Eckstein, T. Eichhorn, G. Flucke, E. Gallo[18], J. Garay Garcia, A. Geiser, A. Gizhko, P. Gunnellini, J. Hauk, M. Hempel[19], H. Jung, A. Kalogeropoulos, O. Karacheban[19], M. Kasemann, P. Katsas, J. Kieseler, C. Kleinwort, I. Korol, W. Lange, J. Leonard, K. Lipka, A. Lobanov, W. Lohmann[19], R. Mankel, I. Marfin[19], I.-A. Melzer-Pellmann, A.B. Meyer, G. Mittag, J. Mnich, A. Mussgiller, S. Naumann-Emme, A. Nayak, E. Ntomari, H. Perrey, D. Pitzl, R. Placakyte, A. Raspereza, B. Roland, M.Ö. Sahin, P. Saxena, T. Schoerner-Sadenius, M. Schröder, C. Seitz, S. Spannagel, K.D. Trippkewitz, R. Walsh, C. Wissing

University of Hamburg, Hamburg, Germany
V. Blobel, M. Centis Vignali, A.R. Draeger, J. Erfle, E. Garutti, K. Goebel, D. Gonzalez, M. Görner, J. Haller, M. Hoffmann, R.S. Höing, A. Junkes, R. Klanner, R. Kogler, T. Lapsien, T. Lenz, I. Marchesini, D. Marconi, M. Meyer, D. Nowatschin, J. Ott, F. Pantaleo[2], T. Peiffer, A. Perieanu, N. Pietsch, J. Poehlsen, D. Rathjens, C. Sander, H. Schettler, P. Schleper, E. Schlieckau, A. Schmidt, J. Schwandt, M. Seidel, V. Sola, H. Stadie, G. Steinbrück, H. Tholen, D. Troendle, E. Usai, L. Vanelderen, A. Vanhoefer, B. Vormwald

Institut für Experimentelle Kernphysik, Karlsruhe, Germany
M. Akbiyik, C. Barth, C. Baus, J. Berger, C. Böser, E. Butz, T. Chwalek, F. Colombo, W. De Boer, A. Descroix, A. Dierlamm, S. Fink, F. Frensch, M. Giffels, A. Gilbert,

JHEP03(2016)125

F. Hartmann[2], S.M. Heindl, U. Husemann, I. Katkov[6], A. Kornmayer[2], P. Lobelle Pardo, B. Maier, H. Mildner, M.U. Mozer, T. Müller, Th. Müller, M. Plagge, G. Quast, K. Rabbertz, S. Röcker, F. Roscher, H.J. Simonis, F.M. Stober, R. Ulrich, J. Wagner-Kuhr, S. Wayand, M. Weber, T. Weiler, C. Wöhrmann, R. Wolf

Institute of Nuclear and Particle Physics (INPP), NCSR Demokritos, Aghia Paraskevi, Greece

G. Anagnostou, G. Daskalakis, T. Geralis, V.A. Giakoumopoulou, A. Kyriakis, D. Loukas, A. Psallidas, I. Topsis-Giotis

University of Athens, Athens, Greece

A. Agapitos, S. Kesisoglou, A. Panagiotou, N. Saoulidou, E. Tziaferi

University of Ioánnina, Ioánnina, Greece

I. Evangelou, G. Flouris, C. Foudas, P. Kokkas, N. Loukas, N. Manthos, I. Papadopoulos, E. Paradas, J. Strologas

Wigner Research Centre for Physics, Budapest, Hungary

G. Bencze, C. Hajdu, A. Hazi, P. Hidas, D. Horvath[20], F. Sikler, V. Veszpremi, G. Vesztergombi[21], A.J. Zsigmond

Institute of Nuclear Research ATOMKI, Debrecen, Hungary

N. Beni, S. Czellar, J. Karancsi[22], J. Molnar, Z. Szillasi

University of Debrecen, Debrecen, Hungary

M. Bartók[23], A. Makovec, P. Raics, Z.L. Trocsanyi, B. Ujvari

National Institute of Science Education and Research, Bhubaneswar, India

P. Mal, K. Mandal, D.K. Sahoo, N. Sahoo, S.K. Swain

Panjab University, Chandigarh, India

S. Bansal, S.B. Beri, V. Bhatnagar, R. Chawla, R. Gupta, U.Bhawandeep, A.K. Kalsi, A. Kaur, M. Kaur, R. Kumar, A. Mehta, M. Mittal, J.B. Singh, G. Walia

University of Delhi, Delhi, India

Ashok Kumar, A. Bhardwaj, B.C. Choudhary, R.B. Garg, A. Kumar, S. Malhotra, M. Naimuddin, N. Nishu, K. Ranjan, R. Sharma, V. Sharma

Saha Institute of Nuclear Physics, Kolkata, India

S. Bhattacharya, K. Chatterjee, S. Dey, S. Dutta, Sa. Jain, N. Majumdar, A. Modak, K. Mondal, S. Mukherjee, S. Mukhopadhyay, A. Roy, D. Roy, S. Roy Chowdhury, S. Sarkar, M. Sharan

Bhabha Atomic Research Centre, Mumbai, India

A. Abdulsalam, R. Chudasama, D. Dutta, V. Jha, V. Kumar, A.K. Mohanty[2], L.M. Pant, P. Shukla, A. Topkar

Tata Institute of Fundamental Research, Mumbai, India

T. Aziz, S. Banerjee, S. Bhowmik[24], R.M. Chatterjee, R.K. Dewanjee, S. Dugad, S. Ganguly, S. Ghosh, M. Guchait, A. Gurtu[25], G. Kole, S. Kumar, B. Mahakud, M. Maity[24],

JHEP03(2016)125

G. Majumder, K. Mazumdar, S. Mitra, G.B. Mohanty, B. Parida, T. Sarkar[24], K. Sudhakar, N. Sur, B. Sutar, N. Wickramage[26]

Indian Institute of Science Education and Research (IISER), Pune, India
S. Chauhan, S. Dube, S. Sharma

Institute for Research in Fundamental Sciences (IPM), Tehran, Iran
H. Bakhshiansohi, H. Behnamian, S.M. Etesami[27], A. Fahim[28], R. Goldouzian, M. Khakzad, M. Mohammadi Najafabadi, M. Naseri, S. Paktinat Mehdiabadi, F. Rezaei Hosseinabadi, B. Safarzadeh[29], M. Zeinali

University College Dublin, Dublin, Ireland
M. Felcini, M. Grunewald

INFN Sezione di Bari [a], Università di Bari [b], Politecnico di Bari [c], Bari, Italy
M. Abbrescia[a,b], C. Calabria[a,b], C. Caputo[a,b], A. Colaleo[a], D. Creanza[a,c], L. Cristella[a,b], N. De Filippis[a,c], M. De Palma[a,b], L. Fiore[a], G. Iaselli[a,c], G. Maggi[a,c], M. Maggi[a], G. Miniello[a,b], S. My[a,c], S. Nuzzo[a,b], A. Pompili[a,b], G. Pugliese[a,c], R. Radogna[a,b], A. Ranieri[a], G. Selvaggi[a,b], L. Silvestris[a,2], R. Venditti[a,b], P. Verwilligen[a]

INFN Sezione di Bologna [a], Università di Bologna [b], Bologna, Italy
G. Abbiendi[a], C. Battilana[2], A.C. Benvenuti[a], D. Bonacorsi[a,b], S. Braibant-Giacomelli[a,b], L. Brigliadori[a,b], R. Campanini[a,b], P. Capiluppi[a,b], A. Castro[a,b], F.R. Cavallo[a], S.S. Chhibra[a,b], G. Codispoti[a,b], M. Cuffiani[a,b], G.M. Dallavalle[a], F. Fabbri[a], A. Fanfani[a,b], D. Fasanella[a,b], P. Giacomelli[a], C. Grandi[a], L. Guiducci[a,b], S. Marcellini[a], G. Masetti[a], A. Montanari[a], F.L. Navarria[a,b], A. Perrotta[a], A.M. Rossi[a,b], T. Rovelli[a,b], G.P. Siroli[a,b], N. Tosi[a,b], R. Travaglini[a,b]

INFN Sezione di Catania [a], Università di Catania [b], Catania, Italy
G. Cappello[a], M. Chiorboli[a,b], S. Costa[a,b], F. Giordano[a,b], R. Potenza[a,b], A. Tricomi[a,b], C. Tuve[a,b]

INFN Sezione di Firenze [a], Università di Firenze [b], Firenze, Italy
G. Barbagli[a], V. Ciulli[a,b], C. Civinini[a], R. D'Alessandro[a,b], E. Focardi[a,b], S. Gonzi[a,b], V. Gori[a,b], P. Lenzi[a,b], M. Meschini[a], S. Paoletti[a], G. Sguazzoni[a], A. Tropiano[a,b], L. Viliani[a,b]

INFN Laboratori Nazionali di Frascati, Frascati, Italy
L. Benussi, S. Bianco, F. Fabbri, D. Piccolo, F. Primavera

INFN Sezione di Genova [a], Università di Genova [b], Genova, Italy
V. Calvelli[a,b], F. Ferro[a], M. Lo Vetere[a,b], M.R. Monge[a,b], E. Robutti[a], S. Tosi[a,b]

INFN Sezione di Milano-Bicocca [a], Università di Milano-Bicocca [b], Milano, Italy
L. Brianza, M.E. Dinardo[a,b], S. Fiorendi[a,b], S. Gennai[a], R. Gerosa[a,b], A. Ghezzi[a,b], P. Govoni[a,b], S. Malvezzi[a], R.A. Manzoni[a,b], B. Marzocchi[a,b,2], D. Menasce[a], L. Moroni[a], M. Paganoni[a,b], D. Pedrini[a], S. Ragazzi[a,b], N. Redaelli[a], T. Tabarelli de Fatis[a,b]

JHEP03(2016)125

INFN Sezione di Napoli [a], Università di Napoli 'Federico II' [b], Napoli, Italy, Università della Basilicata [c], Potenza, Italy, Università G. Marconi [d], Roma, Italy

S. Buontempo[a], N. Cavallo[a,c], S. Di Guida[a,d,2], M. Esposito[a,b], F. Fabozzi[a,c], A.O.M. Iorio[a,b], G. Lanza[a], L. Lista[a], S. Meola[a,d,2], M. Merola[a], P. Paolucci[a,2], C. Sciacca[a,b], F. Thyssen

INFN Sezione di Padova [a], Università di Padova [b], Padova, Italy, Università di Trento [c], Trento, Italy

P. Azzi[a,2], N. Bacchetta[a], L. Benato[a,b], D. Bisello[a,b], A. Boletti[a,b], R. Carlin[a,b], P. Checchia[a], M. Dall'Osso[a,b,2], T. Dorigo[a], S. Fantinel[a], F. Fanzago[a], F. Gasparini[a,b], U. Gasparini[a,b], F. Gonella[a], A. Gozzelino[a], K. Kanishchev[a,c], S. Lacaprara[a], M. Margoni[a,b], A.T. Meneguzzo[a,b], J. Pazzini[a,b], N. Pozzobon[a,b], P. Ronchese[a,b], F. Simonetto[a,b], E. Torassa[a], M. Tosi[a,b], M. Zanetti, P. Zotto[a,b], A. Zucchetta[a,b,2], G. Zumerle[a,b]

INFN Sezione di Pavia [a], Università di Pavia [b], Pavia, Italy

A. Braghieri[a], A. Magnani[a], P. Montagna[a,b], S.P. Ratti[a,b], V. Re[a], C. Riccardi[a,b], P. Salvini[a], I. Vai[a], P. Vitulo[a,b]

INFN Sezione di Perugia [a], Università di Perugia [b], Perugia, Italy

L. Alunni Solestizi[a,b], M. Biasini[a,b], G.M. Bilei[a], D. Ciangottini[a,b,2], L. Fanò[a,b], P. Lariccia[a,b], G. Mantovani[a,b], M. Menichelli[a], A. Saha[a], A. Santocchia[a,b], A. Spiezia[a,b]

INFN Sezione di Pisa [a], Università di Pisa [b], Scuola Normale Superiore di Pisa [c], Pisa, Italy

K. Androsov[a,30], P. Azzurri[a], G. Bagliesi[a], J. Bernardini[a], T. Boccali[a], G. Broccolo[a,c], R. Castaldi[a], M.A. Ciocci[a,30], R. Dell'Orso[a], S. Donato[a,c,2], G. Fedi, L. Foà[a,c†], A. Giassi[a], M.T. Grippo[a,30], F. Ligabue[a,c], T. Lomtadze[a], L. Martini[a,b], A. Messineo[a,b], F. Palla[a], A. Rizzi[a,b], A. Savoy-Navarro[a,31], A.T. Serban[a], P. Spagnolo[a], P. Squillacioti[a,30], R. Tenchini[a], G. Tonelli[a,b], A. Venturi[a], P.G. Verdini[a]

INFN Sezione di Roma [a], Università di Roma [b], Roma, Italy

L. Barone[a,b], F. Cavallari[a], G. D'imperio[a,b,2], D. Del Re[a,b], M. Diemoz[a], S. Gelli[a,b], C. Jorda[a], E. Longo[a,b], F. Margaroli[a,b], P. Meridiani[a], G. Organtini[a,b], R. Paramatti[a], F. Preiato[a,b], S. Rahatlou[a,b], C. Rovelli[a], F. Santanastasio[a,b], P. Traczyk[a,b,2]

INFN Sezione di Torino [a], Università di Torino [b], Torino, Italy, Università del Piemonte Orientale [c], Novara, Italy

N. Amapane[a,b], R. Arcidiacono[a,c,2], S. Argiro[a,b], M. Arneodo[a,c], R. Bellan[a,b], C. Biino[a], N. Cartiglia[a], M. Costa[a,b], R. Covarelli[a,b], P. De Remigis[a], A. Degano[a,b], N. Demaria[a], L. Finco[a,b], B. Kiani[a,b], C. Mariotti[a], S. Maselli[a], E. Migliore[a,b], V. Monaco[a,b], E. Monteil[a,b], M. Musich[a], M.M. Obertino[a,b], L. Pacher[a,b], N. Pastrone[a], M. Pelliccioni[a], G.L. Pinna Angioni[a,b], F. Ravera[a,b], A. Romero[a,b], M. Ruspa[a,c], R. Sacchi[a,b], A. Solano[a,b], A. Staiano[a]

JHEP03(2016)125

INFN Sezione di Trieste [a], Università di Trieste [b], Trieste, Italy
S. Belforte[a], V. Candelise[a,b,2], M. Casarsa[a], F. Cossutti[a], G. Della Ricca[a,b], B. Gobbo[a], C. La Licata[a,b], M. Marone[a,b], A. Schizzi[a,b], A. Zanetti[a]

Kangwon National University, Chunchon, Korea
A. Kropivnitskaya, S.K. Nam

Kyungpook National University, Daegu, Korea
D.H. Kim, G.N. Kim, M.S. Kim, D.J. Kong, S. Lee, Y.D. Oh, A. Sakharov, D.C. Son

Chonbuk National University, Jeonju, Korea
J.A. Brochero Cifuentes, H. Kim, T.J. Kim, M.S. Ryu

Chonnam National University, Institute for Universe and Elementary Particles, Kwangju, Korea
S. Song

Korea University, Seoul, Korea
S. Choi, Y. Go, D. Gyun, B. Hong, M. Jo, H. Kim, Y. Kim, B. Lee, K. Lee, K.S. Lee, S. Lee, S.K. Park, Y. Roh

Seoul National University, Seoul, Korea
H.D. Yoo

University of Seoul, Seoul, Korea
M. Choi, H. Kim, J.H. Kim, J.S.H. Lee, I.C. Park, G. Ryu

Sungkyunkwan University, Suwon, Korea
Y. Choi, J. Goh, D. Kim, E. Kwon, J. Lee, I. Yu

Vilnius University, Vilnius, Lithuania
A. Juodagalvis, J. Vaitkus

National Centre for Particle Physics, Universiti Malaya, Kuala Lumpur, Malaysia
I. Ahmed, Z.A. Ibrahim, J.R. Komaragiri, M.A.B. Md Ali[32], F. Mohamad Idris[33], W.A.T. Wan Abdullah, M.N. Yusli

Centro de Investigacion y de Estudios Avanzados del IPN, Mexico City, Mexico
E. Casimiro Linares, H. Castilla-Valdez, E. De La Cruz-Burelo, I. Heredia-de La Cruz[34], A. Hernandez-Almada, R. Lopez-Fernandez, A. Sanchez-Hernandez

Universidad Iberoamericana, Mexico City, Mexico
S. Carrillo Moreno, F. Vazquez Valencia

Benemerita Universidad Autonoma de Puebla, Puebla, Mexico
I. Pedraza, H.A. Salazar Ibarguen

Universidad Autónoma de San Luis Potosí, San Luis Potosí, Mexico
A. Morelos Pineda

JHEP03(2016)125

University of Auckland, Auckland, New Zealand
D. Krofcheck

University of Canterbury, Christchurch, New Zealand
P.H. Butler

National Centre for Physics, Quaid-I-Azam University, Islamabad, Pakistan
A. Ahmad, M. Ahmad, Q. Hassan, H.R. Hoorani, W.A. Khan, T. Khurshid, M. Shoaib

National Centre for Nuclear Research, Swierk, Poland
H. Bialkowska, M. Bluj, B. Boimska, T. Frueboes, M. Górski, M. Kazana, K. Nawrocki, K. Romanowska-Rybinska, M. Szleper, P. Zalewski

Institute of Experimental Physics, Faculty of Physics, University of Warsaw, Warsaw, Poland
G. Brona, K. Bunkowski, A. Byszuk[35], K. Doroba, A. Kalinowski, M. Konecki, J. Krolikowski, M. Misiura, M. Olszewski, M. Walczak

Laboratório de Instrumentação e Física Experimental de Partículas, Lisboa, Portugal
P. Bargassa, C. Beirão Da Cruz E Silva, A. Di Francesco, P. Faccioli, P.G. Ferreira Parracho, M. Gallinaro, N. Leonardo, L. Lloret Iglesias, F. Nguyen, J. Rodrigues Antunes, J. Seixas, O. Toldaiev, D. Vadruccio, J. Varela, P. Vischia

Joint Institute for Nuclear Research, Dubna, Russia
S. Afanasiev, P. Bunin, M. Gavrilenko, I. Golutvin, I. Gorbunov, A. Kamenev, V. Karjavin, V. Konoplyanikov, A. Lanev, A. Malakhov, V. Matveev[36], P. Moisenz, V. Palichik, V. Perelygin, S. Shmatov, S. Shulha, N. Skatchkov, V. Smirnov, A. Zarubin

Petersburg Nuclear Physics Institute, Gatchina (St. Petersburg), Russia
V. Golovtsov, Y. Ivanov, V. Kim[37], E. Kuznetsova, P. Levchenko, V. Murzin, V. Oreshkin, I. Smirnov, V. Sulimov, L. Uvarov, S. Vavilov, A. Vorobyev

Institute for Nuclear Research, Moscow, Russia
Yu. Andreev, A. Dermenev, S. Gninenko, N. Golubev, A. Karneyeu, M. Kirsanov, N. Krasnikov, A. Pashenkov, D. Tlisov, A. Toropin

Institute for Theoretical and Experimental Physics, Moscow, Russia
V. Epshteyn, V. Gavrilov, N. Lychkovskaya, V. Popov, I. Pozdnyakov, G. Safronov, A. Spiridonov, E. Vlasov, A. Zhokin

National Research Nuclear University 'Moscow Engineering Physics Institute' (MEPhI), Moscow, Russia
A. Bylinkin

P.N. Lebedev Physical Institute, Moscow, Russia
V. Andreev, M. Azarkin[38], I. Dremin[38], M. Kirakosyan, A. Leonidov[38], G. Mesyats, S.V. Rusakov, A. Vinogradov

JHEP03(2016)125

Skobeltsyn Institute of Nuclear Physics, Lomonosov Moscow State University, Moscow, Russia

A. Baskakov, A. Belyaev, E. Boos, V. Bunichev, M. Dubinin[39], L. Dudko, A. Ershov, A. Gribushin, V. Klyukhin, O. Kodolova, I. Lokhtin, I. Myagkov, S. Obraztsov, S. Petrushanko, V. Savrin

State Research Center of Russian Federation, Institute for High Energy Physics, Protvino, Russia

I. Azhgirey, I. Bayshev, S. Bitioukov, V. Kachanov, A. Kalinin, D. Konstantinov, V. Krychkine, V. Petrov, R. Ryutin, A. Sobol, L. Tourtchanovitch, S. Troshin, N. Tyurin, A. Uzunian, A. Volkov

University of Belgrade, Faculty of Physics and Vinca Institute of Nuclear Sciences, Belgrade, Serbia

P. Adzic[40], M. Ekmedzic, J. Milosevic, V. Rekovic

Centro de Investigaciones Energéticas Medioambientales y Tecnológicas (CIEMAT), Madrid, Spain

J. Alcaraz Maestre, E. Calvo, M. Cerrada, M. Chamizo Llatas, N. Colino, B. De La Cruz, A. Delgado Peris, D. Domínguez Vázquez, A. Escalante Del Valle, C. Fernandez Bedoya, J.P. Fernández Ramos, J. Flix, M.C. Fouz, P. Garcia-Abia, O. Gonzalez Lopez, S. Goy Lopez, J.M. Hernandez, M.I. Josa, E. Navarro De Martino, A. Pérez-Calero Yzquierdo, J. Puerta Pelayo, A. Quintario Olmeda, I. Redondo, L. Romero, M.S. Soares

Universidad Autónoma de Madrid, Madrid, Spain

C. Albajar, J.F. de Trocóniz, M. Missiroli, D. Moran

Universidad de Oviedo, Oviedo, Spain

J. Cuevas, J. Fernandez Menendez, S. Folgueras, I. Gonzalez Caballero, E. Palencia Cortezon, J.M. Vizan Garcia

Instituto de Física de Cantabria (IFCA), CSIC-Universidad de Cantabria, Santander, Spain

I.J. Cabrillo, A. Calderon, J.R. Castiñeiras De Saa, P. De Castro Manzano, J. Duarte Campderros, M. Fernandez, J. Garcia-Ferrero, G. Gomez, A. Lopez Virto, J. Marco, R. Marco, C. Martinez Rivero, F. Matorras, F.J. Munoz Sanchez, J. Piedra Gomez, T. Rodrigo, A.Y. Rodríguez-Marrero, A. Ruiz-Jimeno, L. Scodellaro, I. Vila, R. Vilar Cortabitarte

CERN, European Organization for Nuclear Research, Geneva, Switzerland

D. Abbaneo, E. Auffray, G. Auzinger, M. Bachtis, P. Baillon, A.H. Ball, D. Barney, A. Benaglia, J. Bendavid, L. Benhabib, J.F. Benitez, G.M. Berruti, P. Bloch, A. Bocci, A. Bonato, C. Botta, H. Breuker, T. Camporesi, R. Castello, G. Cerminara, S. Colafranceschi[41], M. D'Alfonso, D. d'Enterria, A. Dabrowski, V. Daponte, A. David, M. De Gruttola, F. De Guio, A. De Roeck, S. De Visscher, E. Di Marco, M. Dobson, M. Dordevic, B. Dorney, T. du Pree, M. Dünser, N. Dupont, A. Elliott-Peisert, G. Franzoni, W. Funk, D. Gigi, K. Gill, D. Giordano, M. Girone, F. Glege, R. Guida, S. Gundacker, M. Guthoff, J. Hammer,

JHEP03(2016)125

P. Harris, J. Hegeman, V. Innocente, P. Janot, H. Kirschenmann, M.J. Kortelainen, K. Kousouris, K. Krajczar, P. Lecoq, C. Lourenço, M.T. Lucchini, N. Magini, L. Malgeri, M. Mannelli, A. Martelli, L. Masetti, F. Meijers, S. Mersi, E. Meschi, F. Moortgat, S. Morovic, M. Mulders, M.V. Nemallapudi, H. Neugebauer, S. Orfanelli[42], L. Orsini, L. Pape, E. Perez, M. Peruzzi, A. Petrilli, G. Petrucciani, A. Pfeiffer, D. Piparo, A. Racz, G. Rolandi[43], M. Rovere, M. Ruan, H. Sakulin, C. Schäfer, C. Schwick, A. Sharma, P. Silva, M. Simon, P. Sphicas[44], D. Spiga, J. Steggemann, B. Stieger, M. Stoye, Y. Takahashi, D. Treille, A. Triossi, A. Tsirou, G.I. Veres[21], N. Wardle, H.K. Wöhri, A. Zagozdzinska[35], W.D. Zeuner

Paul Scherrer Institut, Villigen, Switzerland

W. Bertl, K. Deiters, W. Erdmann, R. Horisberger, Q. Ingram, H.C. Kaestli, D. Kotlinski, U. Langenegger, D. Renker, T. Rohe

Institute for Particle Physics, ETH Zurich, Zurich, Switzerland

F. Bachmair, L. Bäni, L. Bianchini, M.A. Buchmann, B. Casal, G. Dissertori, M. Dittmar, M. Donegà, P. Eller, C. Grab, C. Heidegger, D. Hits, J. Hoss, G. Kasieczka, W. Lustermann, B. Mangano, M. Marionneau, P. Martinez Ruiz del Arbol, M. Masciovecchio, D. Meister, F. Micheli, P. Musella, F. Nessi-Tedaldi, F. Pandolfi, J. Pata, F. Pauss, L. Perrozzi, M. Quittnat, M. Rossini, A. Starodumov[45], M. Takahashi, V.R. Tavolaro, K. Theofilatos, R. Wallny

Universität Zürich, Zurich, Switzerland

T.K. Aarrestad, C. Amsler[46], L. Caminada, M.F. Canelli, V. Chiochia, A. De Cosa, C. Galloni, A. Hinzmann, T. Hreus, B. Kilminster, C. Lange, J. Ngadiuba, D. Pinna, P. Robmann, F.J. Ronga, D. Salerno, Y. Yang

National Central University, Chung-Li, Taiwan

M. Cardaci, K.H. Chen, T.H. Doan, Sh. Jain, R. Khurana, M. Konyushikhin, C.M. Kuo, W. Lin, Y.J. Lu, S.H. Mai, S.S. Yu

National Taiwan University (NTU), Taipei, Taiwan

Arun Kumar, R. Bartek, P. Chang, Y.H. Chang, Y.W. Chang, Y. Chao, K.F. Chen, P.H. Chen, C. Dietz, F. Fiori, U. Grundler, W.-S. Hou, Y. Hsiung, Y.F. Liu, R.-S. Lu, M. Miñano Moya, E. Petrakou, J.f. Tsai, Y.M. Tzeng

Chulalongkorn University, Faculty of Science, Department of Physics, Bangkok, Thailand

B. Asavapibhop, K. Kovitanggoon, G. Singh, N. Srimanobhas, N. Suwonjandee

Cukurova University, Adana, Turkey

A. Adiguzel, S. Cerci[47], Z.S. Demiroglu, C. Dozen, I. Dumanoglu, S. Girgis, G. Gokbulut, Y. Guler, E. Gurpinar, I. Hos, E.E. Kangal[48], A. Kayis Topaksu, G. Onengut[49], K. Ozdemir[50], S. Ozturk[51], B. Tali[47], H. Topakli[51], M. Vergili, C. Zorbilmez

Middle East Technical University, Physics Department, Ankara, Turkey

I.V. Akin, B. Bilin, S. Bilmis, B. Isildak[52], G. Karapinar[53], M. Yalvac, M. Zeyrek

JHEP03(2016)125

Bogazici University, Istanbul, Turkey

E.A. Albayrak[54], E. Gülmez, M. Kaya[55], O. Kaya[56], T. Yetkin[57]

Istanbul Technical University, Istanbul, Turkey

K. Cankocak, S. Sen[58], F.I. Vardarlı

Institute for Scintillation Materials of National Academy of Science of Ukraine, Kharkov, Ukraine

B. Grynyov

National Scientific Center, Kharkov Institute of Physics and Technology, Kharkov, Ukraine

L. Levchuk, P. Sorokin

University of Bristol, Bristol, United Kingdom

R. Aggleton, F. Ball, L. Beck, J.J. Brooke, E. Clement, D. Cussans, H. Flacher, J. Goldstein, M. Grimes, G.P. Heath, H.F. Heath, J. Jacob, L. Kreczko, C. Lucas, Z. Meng, D.M. Newbold[59], S. Paramesvaran, A. Poll, T. Sakuma, S. Seif El Nasr-storey, S. Senkin, D. Smith, V.J. Smith

Rutherford Appleton Laboratory, Didcot, United Kingdom

K.W. Bell, A. Belyaev[60], C. Brew, R.M. Brown, D. Cieri, D.J.A. Cockerill, J.A. Coughlan, K. Harder, S. Harper, E. Olaiya, D. Petyt, C.H. Shepherd-Themistocleous, A. Thea, I.R. Tomalin, T. Williams, W.J. Womersley, S.D. Worm

Imperial College, London, United Kingdom

M. Baber, R. Bainbridge, O. Buchmuller, A. Bundock, D. Burton, S. Casasso, M. Citron, D. Colling, L. Corpe, N. Cripps, P. Dauncey, G. Davies, A. De Wit, M. Della Negra, P. Dunne, A. Elwood, W. Ferguson, J. Fulcher, D. Futyan, G. Hall, G. Iles, M. Kenzie, R. Lane, R. Lucas[59], L. Lyons, A.-M. Magnan, S. Malik, J. Nash, A. Nikitenko[45], J. Pela, M. Pesaresi, K. Petridis, D.M. Raymond, A. Richards, A. Rose, C. Seez, A. Tapper, K. Uchida, M. Vazquez Acosta[61], T. Virdee, S.C. Zenz

Brunel University, Uxbridge, United Kingdom

J.E. Cole, P.R. Hobson, A. Khan, P. Kyberd, D. Leggat, D. Leslie, I.D. Reid, P. Symonds, L. Teodorescu, M. Turner

Baylor University, Waco, USA

A. Borzou, K. Call, J. Dittmann, K. Hatakeyama, A. Kasmi, H. Liu, N. Pastika

The University of Alabama, Tuscaloosa, USA

O. Charaf, S.I. Cooper, C. Henderson, P. Rumerio

Boston University, Boston, USA

A. Avetisyan, T. Bose, C. Fantasia, D. Gastler, P. Lawson, D. Rankin, C. Richardson, J. Rohlf, J. St. John, L. Sulak, D. Zou

JHEP03(2016)125

Brown University, Providence, USA

J. Alimena, E. Berry, S. Bhattacharya, D. Cutts, N. Dhingra, A. Ferapontov, A. Garabedian, J. Hakala, U. Heintz, E. Laird, G. Landsberg, Z. Mao, M. Narain, S. Piperov, S. Sagir, T. Sinthuprasith, R. Syarif

University of California, Davis, Davis, USA

R. Breedon, G. Breto, M. Calderon De La Barca Sanchez, S. Chauhan, M. Chertok, J. Conway, R. Conway, P.T. Cox, R. Erbacher, M. Gardner, W. Ko, R. Lander, M. Mulhearn, D. Pellett, J. Pilot, F. Ricci-Tam, S. Shalhout, J. Smith, M. Squires, D. Stolp, M. Tripathi, S. Wilbur, R. Yohay

University of California, Los Angeles, USA

R. Cousins, P. Everaerts, C. Farrell, J. Hauser, M. Ignatenko, D. Saltzberg, E. Takasugi, V. Valuev, M. Weber

University of California, Riverside, Riverside, USA

K. Burt, R. Clare, J. Ellison, J.W. Gary, G. Hanson, J. Heilman, M. Ivova PANEVA, P. Jandir, E. Kennedy, F. Lacroix, O.R. Long, A. Luthra, M. Malberti, M. Olmedo Negrete, A. Shrinivas, H. Wei, S. Wimpenny, B. R. Yates

University of California, San Diego, La Jolla, USA

J.G. Branson, G.B. Cerati, S. Cittolin, R.T. D'Agnolo, A. Holzner, R. Kelley, D. Klein, J. Letts, I. Macneill, D. Olivito, S. Padhi, M. Pieri, M. Sani, V. Sharma, S. Simon, M. Tadel, A. Vartak, S. Wasserbaech[62], C. Welke, F. Würthwein, A. Yagil, G. Zevi Della Porta

University of California, Santa Barbara, Santa Barbara, USA

D. Barge, J. Bradmiller-Feld, C. Campagnari, A. Dishaw, V. Dutta, K. Flowers, M. Franco Sevilla, P. Geffert, C. George, F. Golf, L. Gouskos, J. Gran, J. Incandela, C. Justus, N. Mccoll, S.D. Mullin, J. Richman, D. Stuart, I. Suarez, W. To, C. West, J. Yoo

California Institute of Technology, Pasadena, USA

D. Anderson, A. Apresyan, A. Bornheim, J. Bunn, Y. Chen, J. Duarte, A. Mott, H.B. Newman, C. Pena, M. Pierini, M. Spiropulu, J.R. Vlimant, S. Xie, R.Y. Zhu

Carnegie Mellon University, Pittsburgh, USA

M.B. Andrews, V. Azzolini, A. Calamba, B. Carlson, T. Ferguson, M. Paulini, J. Russ, M. Sun, H. Vogel, I. Vorobiev

University of Colorado Boulder, Boulder, USA

J.P. Cumalat, W.T. Ford, A. Gaz, F. Jensen, A. Johnson, M. Krohn, T. Mulholland, U. Nauenberg, K. Stenson, S.R. Wagner

Cornell University, Ithaca, USA

J. Alexander, A. Chatterjee, J. Chaves, J. Chu, S. Dittmer, N. Eggert, N. Mirman, G. Nicolas Kaufman, J.R. Patterson, A. Rinkevicius, A. Ryd, L. Skinnari, L. Soffi, W. Sun, S.M. Tan, W.D. Teo, J. Thom, J. Thompson, J. Tucker, Y. Weng, P. Wittich

JHEP03(2016)125

Fermi National Accelerator Laboratory, Batavia, USA
S. Abdullin, M. Albrow, J. Anderson, G. Apollinari, S. Banerjee, L.A.T. Bauerdick, A. Beretvas, J. Berryhill, P.C. Bhat, G. Bolla, K. Burkett, J.N. Butler, H.W.K. Cheung, F. Chlebana, S. Cihangir, V.D. Elvira, I. Fisk, J. Freeman, E. Gottschalk, L. Gray, D. Green, S. Grünendahl, O. Gutsche, J. Hanlon, D. Hare, R.M. Harris, S. Hasegawa, J. Hirschauer, Z. Hu, S. Jindariani, M. Johnson, U. Joshi, A.W. Jung, B. Klima, B. Kreis, S. Kwan[†], S. Lammel, J. Linacre, D. Lincoln, R. Lipton, T. Liu, R. Lopes De Sá, J. Lykken, K. Maeshima, J.M. Marraffino, V.I. Martinez Outschoorn, S. Maruyama, D. Mason, P. McBride, P. Merkel, K. Mishra, S. Mrenna, S. Nahn, C. Newman-Holmes, V. O'Dell, K. Pedro, O. Prokofyev, G. Rakness, E. Sexton-Kennedy, A. Soha, W.J. Spalding, L. Spiegel, L. Taylor, S. Tkaczyk, N.V. Tran, L. Uplegger, E.W. Vaandering, C. Vernieri, M. Verzocchi, R. Vidal, H.A. Weber, A. Whitbeck, F. Yang

University of Florida, Gainesville, USA
D. Acosta, P. Avery, P. Bortignon, D. Bourilkov, A. Carnes, M. Carver, D. Curry, S. Das, G.P. Di Giovanni, R.D. Field, I.K. Furic, J. Hugon, J. Konigsberg, A. Korytov, J.F. Low, P. Ma, K. Matchev, H. Mei, P. Milenovic[63], G. Mitselmakher, D. Rank, R. Rossin, L. Shchutska, M. Snowball, D. Sperka, N. Terentyev, L. Thomas, J. Wang, S. Wang, J. Yelton

Florida International University, Miami, USA
S. Hewamanage, S. Linn, P. Markowitz, G. Martinez, J.L. Rodriguez

Florida State University, Tallahassee, USA
A. Ackert, J.R. Adams, T. Adams, A. Askew, J. Bochenek, B. Diamond, J. Haas, S. Hagopian, V. Hagopian, K.F. Johnson, A. Khatiwada, H. Prosper, M. Weinberg

Florida Institute of Technology, Melbourne, USA
M.M. Baarmand, V. Bhopatkar, M. Hohlmann, H. Kalakhety, D. Noonan, T. Roy, F. Yumiceva

University of Illinois at Chicago (UIC), Chicago, USA
M.R. Adams, L. Apanasevich, D. Berry, R.R. Betts, I. Bucinskaite, R. Cavanaugh, O. Evdokimov, L. Gauthier, C.E. Gerber, D.J. Hofman, P. Kurt, C. O'Brien, I.D. Sandoval Gonzalez, C. Silkworth, P. Turner, N. Varelas, Z. Wu, M. Zakaria

The University of Iowa, Iowa City, USA
B. Bilki[64], W. Clarida, K. Dilsiz, S. Durgut, R.P. Gandrajula, M. Haytmyradov, V. Khristenko, J.-P. Merlo, H. Mermerkaya[65], A. Mestvirishvili, A. Moeller, J. Nachtman, H. Ogul, Y. Onel, F. Ozok[54], A. Penzo, C. Snyder, P. Tan, E. Tiras, J. Wetzel, K. Yi

Johns Hopkins University, Baltimore, USA
I. Anderson, B.A. Barnett, B. Blumenfeld, D. Fehling, L. Feng, A.V. Gritsan, P. Maksimovic, C. Martin, M. Osherson, M. Swartz, M. Xiao, Y. Xin, C. You

The University of Kansas, Lawrence, USA
P. Baringer, A. Bean, G. Benelli, C. Bruner, R.P. Kenny III, D. Majumder, M. Malek, M. Murray, S. Sanders, R. Stringer, Q. Wang

JHEP03(2016)125

Kansas State University, Manhattan, USA

A. Ivanov, K. Kaadze, S. Khalil, M. Makouski, Y. Maravin, A. Mohammadi, L.K. Saini, N. Skhirtladze, S. Toda

Lawrence Livermore National Laboratory, Livermore, USA

D. Lange, F. Rebassoo, D. Wright

University of Maryland, College Park, USA

C. Anelli, A. Baden, O. Baron, A. Belloni, B. Calvert, S.C. Eno, C. Ferraioli, J.A. Gomez, N.J. Hadley, S. Jabeen, R.G. Kellogg, T. Kolberg, J. Kunkle, Y. Lu, A.C. Mignerey, Y.H. Shin, A. Skuja, M.B. Tonjes, S.C. Tonwar

Massachusetts Institute of Technology, Cambridge, USA

A. Apyan, R. Barbieri, A. Baty, K. Bierwagen, S. Brandt, W. Busza, I.A. Cali, Z. Demiragli, L. Di Matteo, G. Gomez Ceballos, M. Goncharov, D. Gulhan, Y. Iiyama, G.M. Innocenti, M. Klute, D. Kovalskyi, Y.S. Lai, Y.-J. Lee, A. Levin, P.D. Luckey, A.C. Marini, C. Mcginn, C. Mironov, X. Niu, C. Paus, D. Ralph, C. Roland, G. Roland, J. Salfeld-Nebgen, G.S.F. Stephans, K. Sumorok, M. Varma, D. Velicanu, J. Veverka, J. Wang, T.W. Wang, B. Wyslouch, M. Yang, V. Zhukova

University of Minnesota, Minneapolis, USA

B. Dahmes, A. Evans, A. Finkel, A. Gude, P. Hansen, S. Kalafut, S.C. Kao, K. Klapoetke, Y. Kubota, Z. Lesko, J. Mans, S. Nourbakhsh, N. Ruckstuhl, R. Rusack, N. Tambe, J. Turkewitz

University of Mississippi, Oxford, USA

J.G. Acosta, S. Oliveros

University of Nebraska-Lincoln, Lincoln, USA

E. Avdeeva, K. Bloom, S. Bose, D.R. Claes, A. Dominguez, C. Fangmeier, R. Gonzalez Suarez, R. Kamalieddin, J. Keller, D. Knowlton, I. Kravchenko, J. Lazo-Flores, F. Meier, J. Monroy, F. Ratnikov, J.E. Siado, G.R. Snow

State University of New York at Buffalo, Buffalo, USA

M. Alyari, J. Dolen, J. George, A. Godshalk, C. Harrington, I. Iashvili, J. Kaisen, A. Kharchilava, A. Kumar, S. Rappoccio

Northeastern University, Boston, USA

G. Alverson, E. Barberis, D. Baumgartel, M. Chasco, A. Hortiangtham, A. Massironi, D.M. Morse, D. Nash, T. Orimoto, R. Teixeira De Lima, D. Trocino, R.-J. Wang, D. Wood, J. Zhang

Northwestern University, Evanston, USA

K.A. Hahn, A. Kubik, N. Mucia, N. Odell, B. Pollack, A. Pozdnyakov, M. Schmitt, S. Stoynev, K. Sung, M. Trovato, M. Velasco

JHEP03(2016)125

University of Notre Dame, Notre Dame, USA

A. Brinkerhoff, N. Dev, M. Hildreth, C. Jessop, D.J. Karmgard, N. Kellams, K. Lannon, S. Lynch, N. Marinelli, F. Meng, C. Mueller, Y. Musienko[36], T. Pearson, M. Planer, A. Reinsvold, R. Ruchti, G. Smith, S. Taroni, N. Valls, M. Wayne, M. Wolf, A. Woodard

The Ohio State University, Columbus, USA

L. Antonelli, J. Brinson, B. Bylsma, L.S. Durkin, S. Flowers, A. Hart, C. Hill, R. Hughes, W. Ji, K. Kotov, T.Y. Ling, B. Liu, W. Luo, D. Puigh, M. Rodenburg, B.L. Winer, H.W. Wulsin

Princeton University, Princeton, USA

O. Driga, P. Elmer, J. Hardenbrook, P. Hebda, S.A. Koay, P. Lujan, D. Marlow, T. Medvedeva, M. Mooney, J. Olsen, C. Palmer, P. Piroué, X. Quan, H. Saka, D. Stickland, C. Tully, J.S. Werner, A. Zuranski

University of Puerto Rico, Mayaguez, USA

S. Malik

Purdue University, West Lafayette, USA

V.E. Barnes, D. Benedetti, D. Bortoletto, L. Gutay, M.K. Jha, M. Jones, K. Jung, D.H. Miller, N. Neumeister, B.C. Radburn-Smith, X. Shi, I. Shipsey, D. Silvers, J. Sun, A. Svyatkovskiy, F. Wang, W. Xie, L. Xu

Purdue University Calumet, Hammond, USA

N. Parashar, J. Stupak

Rice University, Houston, USA

A. Adair, B. Akgun, Z. Chen, K.M. Ecklund, F.J.M. Geurts, M. Guilbaud, W. Li, B. Michlin, M. Northup, B.P. Padley, R. Redjimi, J. Roberts, J. Rorie, Z. Tu, J. Zabel

University of Rochester, Rochester, USA

B. Betchart, A. Bodek, P. de Barbaro, R. Demina, Y. Eshaq, T. Ferbel, M. Galanti, A. Garcia-Bellido, J. Han, A. Harel, O. Hindrichs, A. Khukhunaishvili, G. Petrillo, M. Verzetti

The Rockefeller University, New York, USA

L. Demortier

Rutgers, The State University of New Jersey, Piscataway, USA

S. Arora, A. Barker, J.P. Chou, C. Contreras-Campana, E. Contreras-Campana, D. Duggan, D. Ferencek, Y. Gershtein, R. Gray, E. Halkiadakis, D. Hidas, E. Hughes, S. Kaplan, R. Kunnawalkam Elayavalli, A. Lath, K. Nash, S. Panwalkar, M. Park, S. Salur, S. Schnetzer, D. Sheffield, S. Somalwar, R. Stone, S. Thomas, P. Thomassen, M. Walker

University of Tennessee, Knoxville, USA

M. Foerster, G. Riley, K. Rose, S. Spanier, A. York

JHEP03(2016)125

Texas A&M University, College Station, USA

O. Bouhali[66], A. Castaneda Hernandez[66], M. Dalchenko, M. De Mattia, A. Delgado, S. Dildick, R. Eusebi, W. Flanagan, J. Gilmore, T. Kamon[67], V. Krutelyov, R. Mueller, I. Osipenkov, Y. Pakhotin, R. Patel, A. Perloff, A. Rose, A. Safonov, A. Tatarinov, K.A. Ulmer[2]

Texas Tech University, Lubbock, USA

N. Akchurin, C. Cowden, J. Damgov, C. Dragoiu, P.R. Dudero, J. Faulkner, S. Kunori, K. Lamichhane, S.W. Lee, T. Libeiro, S. Undleeb, I. Volobouev

Vanderbilt University, Nashville, USA

E. Appelt, A.G. Delannoy, S. Greene, A. Gurrola, R. Janjam, W. Johns, C. Maguire, Y. Mao, A. Melo, H. Ni, P. Sheldon, B. Snook, S. Tuo, J. Velkovska, Q. Xu

University of Virginia, Charlottesville, USA

M.W. Arenton, S. Boutle, B. Cox, B. Francis, J. Goodell, R. Hirosky, A. Ledovskoy, H. Li, C. Lin, C. Neu, X. Sun, Y. Wang, E. Wolfe, J. Wood, F. Xia

Wayne State University, Detroit, USA

C. Clarke, R. Harr, P.E. Karchin, C. Kottachchi Kankanamge Don, P. Lamichhane, J. Sturdy

University of Wisconsin - Madison, Madison, WI, USA

D.A. Belknap, D. Carlsmith, M. Cepeda, A. Christian, S. Dasu, L. Dodd, S. Duric, E. Friis, B. Gomber, M. Grothe, R. Hall-Wilton, M. Herndon, A. Hervé, P. Klabbers, A. Lanaro, A. Levine, K. Long, R. Loveless, A. Mohapatra, I. Ojalvo, T. Perry, G.A. Pierro, G. Polese, T. Ruggles, T. Sarangi, A. Savin, A. Sharma, N. Smith, W.H. Smith, D. Taylor, N. Woods

JHEP03(2016)125

†: Deceased

1: Also at Vienna University of Technology, Vienna, Austria

2: Also at CERN, European Organization for Nuclear Research, Geneva, Switzerland

3: Also at State Key Laboratory of Nuclear Physics and Technology, Peking University, Beijing, China

4: Also at Institut Pluridisciplinaire Hubert Curien, Université de Strasbourg, Université de Haute Alsace Mulhouse, CNRS/IN2P3, Strasbourg, France

5: Also at National Institute of Chemical Physics and Biophysics, Tallinn, Estonia

6: Also at Skobeltsyn Institute of Nuclear Physics, Lomonosov Moscow State University, Moscow, Russia

7: Also at Universidade Estadual de Campinas, Campinas, Brazil

8: Also at Centre National de la Recherche Scientifique (CNRS) - IN2P3, Paris, France

9: Also at Laboratoire Leprince-Ringuet, Ecole Polytechnique, IN2P3-CNRS, Palaiseau, France

10: Also at Joint Institute for Nuclear Research, Dubna, Russia

11: Now at Suez University, Suez, Egypt

12: Now at British University in Egypt, Cairo, Egypt

13: Also at Cairo University, Cairo, Egypt

14: Also at Fayoum University, El-Fayoum, Egypt
15: Also at Université de Haute Alsace, Mulhouse, France
16: Also at Tbilisi State University, Tbilisi, Georgia
17: Also at Ilia State University, Tbilisi, Georgia
18: Also at University of Hamburg, Hamburg, Germany
19: Also at Brandenburg University of Technology, Cottbus, Germany
20: Also at Institute of Nuclear Research ATOMKI, Debrecen, Hungary
21: Also at Eötvös Loránd University, Budapest, Hungary
22: Also at University of Debrecen, Debrecen, Hungary
23: Also at Wigner Research Centre for Physics, Budapest, Hungary
24: Also at University of Visva-Bharati, Santiniketan, India
25: Now at King Abdulaziz University, Jeddah, Saudi Arabia
26: Also at University of Ruhuna, Matara, Sri Lanka
27: Also at Isfahan University of Technology, Isfahan, Iran
28: Also at University of Tehran, Department of Engineering Science, Tehran, Iran
29: Also at Plasma Physics Research Center, Science and Research Branch, Islamic Azad University, Tehran, Iran
30: Also at Università degli Studi di Siena, Siena, Italy
31: Also at Purdue University, West Lafayette, USA
32: Also at International Islamic University of Malaysia, Kuala Lumpur, Malaysia
33: Also at Malaysian Nuclear Agency, MOSTI, Kajang, Malaysia
34: Also at Consejo Nacional de Ciencia y Tecnología, Mexico city, Mexico
35: Also at Warsaw University of Technology, Institute of Electronic Systems, Warsaw, Poland
36: Also at Institute for Nuclear Research, Moscow, Russia
37: Also at St. Petersburg State Polytechnical University, St. Petersburg, Russia
38: Also at National Research Nuclear University 'Moscow Engineering Physics Institute' (MEPhI), Moscow, Russia
39: Also at California Institute of Technology, Pasadena, USA
40: Also at Faculty of Physics, University of Belgrade, Belgrade, Serbia
41: Also at Facoltà Ingegneria, Università di Roma, Roma, Italy
42: Also at National Technical University of Athens, Athens, Greece
43: Also at Scuola Normale e Sezione dell'INFN, Pisa, Italy
44: Also at University of Athens, Athens, Greece
45: Also at Institute for Theoretical and Experimental Physics, Moscow, Russia
46: Also at Albert Einstein Center for Fundamental Physics, Bern, Switzerland
47: Also at Adiyaman University, Adiyaman, Turkey
48: Also at Mersin University, Mersin, Turkey
49: Also at Cag University, Mersin, Turkey
50: Also at Piri Reis University, Istanbul, Turkey
51: Also at Gaziosmanpasa University, Tokat, Turkey
52: Also at Ozyegin University, Istanbul, Turkey
53: Also at Izmir Institute of Technology, Izmir, Turkey
54: Also at Mimar Sinan University, Istanbul, Istanbul, Turkey
55: Also at Marmara University, Istanbul, Turkey
56: Also at Kafkas University, Kars, Turkey
57: Also at Yildiz Technical University, Istanbul, Turkey
58: Also at Hacettepe University, Ankara, Turkey
59: Also at Rutherford Appleton Laboratory, Didcot, United Kingdom

JHEP03(2016)125

60: Also at School of Physics and Astronomy, University of Southampton, Southampton, United Kingdom
61: Also at Instituto de Astrofísica de Canarias, La Laguna, Spain
62: Also at Utah Valley University, Orem, USA
63: Also at University of Belgrade, Faculty of Physics and Vinca Institute of Nuclear Sciences, Belgrade, Serbia
64: Also at Argonne National Laboratory, Argonne, USA
65: Also at Erzincan University, Erzincan, Turkey
66: Also at Texas A&M University at Qatar, Doha, Qatar
67: Also at Kyungpook National University, Daegu, Korea

JHEP03(2016)125